NJC

RSC Publishing

PAPER

View Article Online
View Journal

Cite this: DOI: 10.1039/c3nj00833a

Octupolar chimeric compounds built from quinoline caged acetate moieties: a novel approach for 2-photon uncaging of biomolecules†

Sébastien Picard,[a] Emilie Genin,[a] Guillaume Clermont,[a] Vincent Hugues,[a] Olivier Mongin[b] and Mireille Blanchard-Desce*[a]

Received (in Montpellier, France) 25th July 2013,
Accepted 3rd September 2013

DOI: 10.1039/c3nj00833a

www.rsc.org/njc

The present study describes the synthesis and investigation of chimeric structures where 6-quinoline and 8-quinoline caging units are integrated in multipolar systems to yield ''hybrid'' molecular structures for two-photon uncaging. These systems were demonstrated to exhibit strikingly enhanced (up to more than 2 orders of magnitude larger for octupolar derivatives) two-photon absorption responses in the NIR region compared to common caging groups. Whereas the quadrupolar compound shows the lowest two-photon uncaging cross-section (δ_u), octupolar chimeric derivatives display one-order larger δ_u values than their dipolar analogues. This opens a promising route for the design of efficient octupolar type derivatives for two-photon uncaging of biomolecules.

Introduction

The use of light as an external trigger offers a number of advantages and has been widely applied in the past decades both in multistep organic synthesis and in biology with ''caged compounds''.[1] Actually light has proven to be an invaluable tool in organic synthesis (especially in solid-phase synthesis) allowing the removal of protecting groups under neutral conditions, without requiring additional chemical reagents. This has been particularly useful to overcome some of the problems associated with extremely sensitive targets, not compatible with acids or bases.[2] Photochemically removable protecting groups also have the advantage to be selectively cleaved in the presence of other conventional protecting groups that are insensitive to light. Moreover, possible differentiation between two photolabile protecting groups based on the fine tuning of the irradiation wavelength led to the concept of chromatic orthogonality.[3] The use of phototriggers has also emerged as a particularly attractive tool for the control and investigation of fundamental biochemical processes. This includes photorelease of biomolecules, photoswitching and optogenetics.[4] The use of a light pulse as the triggering event allows fine temporal control and high selectivity, while it circumvents the use of external reagents in cells and living organisms. Numerous examples of photo-induced release (also termed ''uncaging'') of various active molecules have been reported using standard excitation (*i.e.* one-photon), leading to a well-established list of associated requirements.[4a–c] The uncaging process should be both efficient and fast (especially for applications in neurosciences), produce non-toxic by-products while the photoactivatable precursor (the so-called ''caged'' compound) should display suitable stability in the dark and repressed biological activity.

More recently, two-photon (2P) excitation has gained increasing popularity in this field, due to the many advantages it provides.[4d,f] These include an intrinsic 3D resolution when used in microscopy (*i.e.* focused light). In addition, the use of near-IR excitation wavelengths (instead of one-photon excitation in the UV-blue visible region) leads to increased penetration depth and can be less photo-toxic. The important criterion in the case of 2P uncaging is the 2P sensitivity of caged molecules. This is quantified by the corresponding 2P uncaging action cross-section ($\delta_u = \sigma_2 Q_u$), which is the product of the 2P absorption cross-section (σ_2) and of the uncaging quantum yield (Q_u). Low δ_u values require the use of high excitation intensities which can be detrimental to the biological media. Conversely large δ_u values pave the way for more efficient and less damaging 2P uncaging under biological conditions. In that perspective, δ_u values higher than 3 Goeppert-Mayer (GM) have been suggested as highly desirable for biological applications.[5] This realisation has prompted the quest for novel uncaging structures combining a large 2P absorption cross-section and suitable uncaging efficiency. Yet 2P uncaging is still in the early

[a] Univ. Bordeaux, Institut des Sciences Moléculaires, CNRS UMR 5255, 351 Cours de la Libération, F-33405 Talence Cedex, France. E-mail: m.blanchard-desce@ism.u-bordeaux1.fr; Fax: +33 5-40-00-69-94
[b] Institut des Sciences Chimiques de Rennes, CNRS UMR 6226, Université de Rennes 1, Campus de Beaulieu, 35042 Rennes Cedex, France

† Electronic supplementary information (ESI) available. See DOI: 10.1039/c3nj00833a

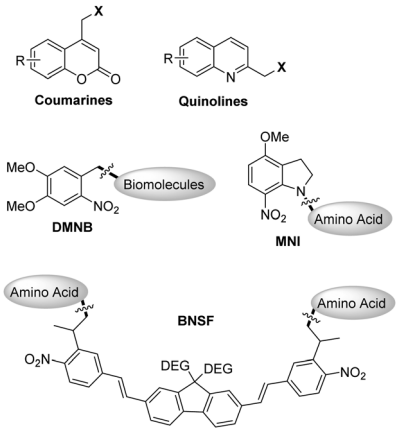

Fig. 1 Selected examples of TP photoactivable cages.

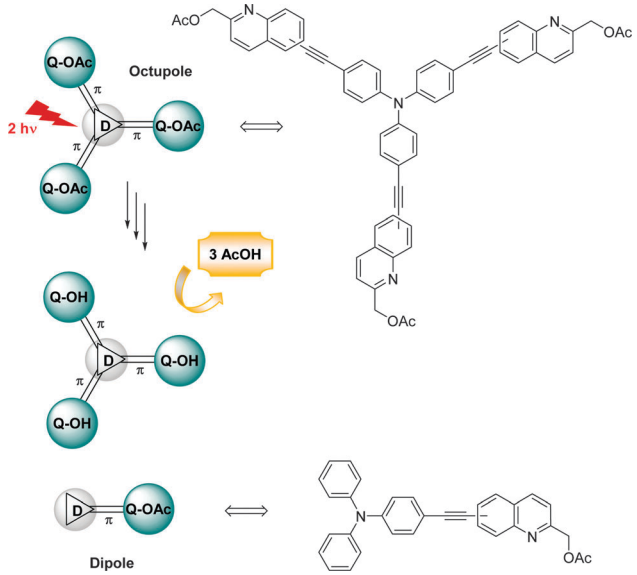

Fig. 2 Octupolar chimeric phototriggers built from a donor triphenylamine core linked to acceptor quinoline caging moieties through an ethynyl spacer and their dipolar analogues.

stages and current cages suitable for efficient 2P photolysis are only scarce (Fig. 1).

Most of the studies reported in the literature up to now have focussed on the investigation and structural modification of common uncaging systems, initially optimised for near-UV excitation. These structures can be classified into different series: widely used nitrophenylalkyl-based cages (δ_u ranging from 0.01 to 3.1 GM), coumarin-4-ylmethyl series (δ_u = 0.35–3.1 GM), quinoline derivatives (δ_u up to 0.9 GM), nitroindoline analogues (δ_u up to 0.06 GM), hydroxycinnamyl cages (δ_u = 0.3–4.7 GM) and ruthenium bipyridyl complexes (δ_u = 0.01–0.1 GM).[1] Very recently, modification of the donor group in biphenyl derivatives in the nitro aromatic series appeared to be quite successful and led to unprecedented δ_u values (up to 11 GM).[6] This successful strategy, based on using dipolar-based compounds for enhancing the 2PA response,[7] was also applied to quadrupolar-based derivatives by Goeldner and co-workers by designing a caging system based on a fluorenyl core bearing two nitroaryl end-groups (BNSF) leading to large δ_u values (5 GM).[8] These results provided evidence that molecular engineering of novel cages by enhancing the 2PA response in multipolar (*i.e.* dipolar or quadrupolar) derivatives is a promising strategy.

Following this line, we decided to investigate an alternative route based on the design of octupolar, rather than quadrupolar, derivatives for 2P uncaging. We chose to focus on dipolar and octupolar derivatives built from a triphenylamine electron-donating moiety linked to electron-withdrawing quinoline caging moieties *via* an ethynyl spacer (Fig. 2). We named these structures "chimeric derivatives" as they are composed of parts taken from two different types of molecules (*i.e.* a triphenylamine-based chromophore and a quinoline-based cage). As demonstrated in earlier studies, triphenylamine-cored octupolar chromophores can combine broad and intense two-photon absorption in the NIR region.[9] This originates from the effective coherent coupling between the dipolar branches which is responsible for the intense 2PA band located at higher energy (corresponding to an electronic state which is one-photon forbidden but strongly two-photon allowed) than that corresponding to the lower excited state (both one and two-photon allowed as in isolated dipolar branches).[10] Taking advantage of the earlier work on the caging activity of quinoline derivatives and related studies emphasising the influence of the substituents (nature and position) on the 2PA response and uncaging efficiency of the quinoline moiety,[11] we investigated structures where the ethynyl spacer is grafted either at the 6- or 8-position. Acetic acid was used as the caged (bio)molecule, allowing easy monitoring of phototriggered release. For comparison purpose and evaluation of the potential benefit of the octupolar approach, we also investigated a quadrupolar analogue built from a fluorenyl core and having similar linkers. We herein report the synthesis and detailed study of the photophysical properties of the series of dipolar, quadrupolar and octupolar chimeric derivatives as well as their ability to release acetic acid under one and 2P excitation in various media. Results are discussed in terms of structure–property relationships.

Results and discussion

Synthesis

6-Substituted quinoline based dipolar and octupolar derivatives (compounds **6** and **8**, respectively) were prepared by means of a Pd(0)-catalysed Sonogashira cross-coupling reaction between (4-iodophenyl)diphenylamine or tris(4-iodophenyl)amine core, respectively, and 6-ethynylquinoline derivative **3** (Scheme 1).

The synthesis of the key intermediate **3** was achieved with a satisfactory overall yield of 68% (in pure isolated compound) following a four-step sequence starting from the commercially available 6-bromo-2-methylquinoline **1**. Compound **1** was converted by a known sequential two-step synthetic procedure[11a,c,h,12] involving oxidation with selenium dioxide followed by the reduction of the intermediate aldehyde using sodium borohydride which leads to the corresponding hydroxymethylene derivative **2**

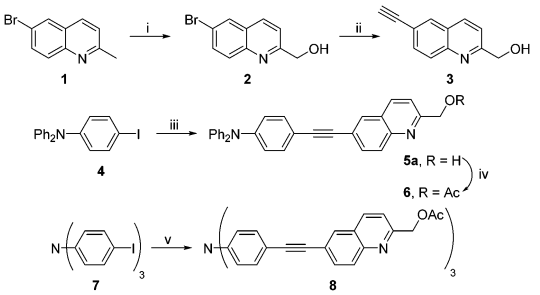

Scheme 1 Reagents and conditions: (i) (a) SeO_2 (1.3 equiv.), dioxane reflux 3 h; (b) $NaBH_4$ (2.0 equiv.), MeOH, 0 °C to RT, overnight, 86% (over 2 steps); (ii) ethynyltrimethylsilane (1.5 equiv.), $PdCl_2(Ph_3P)_2$ (0.05 equiv.), CuI (0.05 equiv.), Ph_3P (0.2 equiv.), toluene–Et_3N (5 : 1), 60 °C, 16 h, then *in situ* at RT, TBAF (1 M in THF, 2.0 equiv.), 2 h, 79% (2 steps); (iii) **3** (1.2 equiv.), $PdCl_2(Ph_3P)_2$ (0.06 equiv.), CuI (0.12 equiv.), THF–Et_3N (5 : 1), RT, 2 h, 84%; (iv) DMAP (0.1 equiv.), Et_3N (2.0 equiv.), Ac_2O (2.0 equiv.), CH_2Cl_2, RT, 4 h, 99%; (v) **3** (3.6 equiv.), $PdCl_2(Ph_3P)_2$ (0.06 equiv.), CuI (0.12 equiv.), THF–Et_3N (5 : 1), RT, 2 h, then *in situ*, DMAP (0.1 equiv.), Ac_2O (2.0 equiv.), RT, 2 h, 94%.

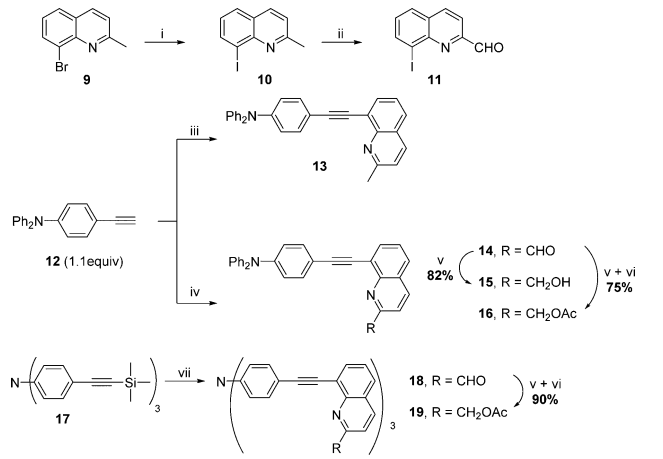

Scheme 2 Reagents and conditions: (i) *n*-BuLi (1.1 equiv.), THF, −70 °C, 1 h, then I_2, −70 °C to rt, 97%; (ii) SeO_2 (1.2 equiv.), dioxane 80 °C, 3 h, 91%; (iii) **10** (1.0 equiv.), $Pd_2(dba)_3$ (0.05 equiv.), CuI (0.1 equiv.), Ph_3P (0.2 equiv.), THF–Et_3N (20 : 1), RT, 3 h, 12%; (iv) **11** (1.0 equiv.), $Pd_2(dba)_3$ (0.05 equiv.), CuI (0.1 equiv.), Ph_3P (0.2 equiv.), THF–Et_3N (20 : 1), RT, 3 h, 51%; (v) $NaBH_4$, THF, RT, overnight; (vi) DMAP (0.1 equiv.), Ac_2O : Et_3N (1 : 1, v/v); (vii) **11** (3.3 equiv.), $Pd_2(dba)_3$ (0.05 equiv.), CuI (0.1 equiv.), Ph_3P (0.2 equiv.), TBAF (3.3 equiv.), THF–Et_3N (5 : 1), RT, overnight, 47%.

with an excellent yield (86%). Further Sonogashira coupling reaction with ethynyltrimethylsilane, followed by a deprotection, *in situ*, of the trimethylsilane group by addition of a solution of tetrabutylammonium fluoride provided the 6-ethynylquinoline molecule **3** very efficiently (79%). **3** was subsequently transformed into compound **5a** *via* a Sonogashira coupling reaction with the known (4-iodophenyl)diphenylamine[13] **4** with 84% yield. Next, treatment of the resulting alcohol **5a** with acetic anhydride led quantitatively to the dipolar 6-substituted quinoline caged acetate **6**. Following the same strategy and starting from the known tris-(4-iodophenyl)amine[14] **7**, we conducted an efficient one-pot two-step sequence involving a threefold Sonogashira coupling followed, *in situ*, by the acetylation reaction to access the octupolar caged acetate **8**. This modification of the initial route was required due to the very low solubility of the intermediate triol in common organic solvents, which hinders its isolation, purification and further conversion.

Keeping in mind that the position of the substituent on the quinoline moiety might influence the photochemical and photophysical properties of the cage, we also prepared quinoline based dipolar and octupolar derivatives substituted at the 8-position (**16** and **19**). In fact, it has been very recently reported that 8-(*N*,*N*-dimethylamino)quinoline (DMAQ) is considerably more sensitive to 2P photolysis than its 6-DMAQ analogue.[11h] In the course of the synthesis, we noticed an important difference of reactivity between the 6-substituted and 8-substituted derivatives that brought us to rethink the synthetic route detailed above and successfully applied for the 6-substituted derivatives (Scheme 2).

We thus prepared the 8-iodoquinoline-2-carboxaldehyde **11** in two steps from the commercially available 8-bromoquinaldine **9**. First, treatment of compound **9** with *n*-butyllithium followed by the quenching of the metalated intermediate with a diode gave rise to an efficient exchange of the bromide atom with an iodide atom and provided 8-iodoquinaldine **10** with 97% yield. Classical oxidation with selenium oxide then afforded the corresponding aldehyde **11** with 91% yield. Parallel to the synthesis of caged acetate, the synthesis of a reference, non-photoactivatable compound was performed for comparison purpose. The preparation of compound **13** was achieved *via* a Sonogashira coupling between *N*-(4-ethynylphenyl)-*N*,*N*-diphenylamine[15] **12** and quinaldine **10** in the presence of $Pd_2(dba)_3$, triphenylphosphine and CuI in THF–Et_3N. The dipolar aldehyde **14** was obtained similarly from alkyne **12** and 8-iodoquinoline-2-carboxaldehyde **11** with a reasonable yield (51%). The aldehyde functional group was reduced into the corresponding alcohol in the presence of $NaBH_4$ and then the acetyl group was introduced. The dipolar 8-substituted quinoline caged acetate **16** was synthesised in two steps from its precursor **14** with a good overall yield (75%). The octupolar 8-substituted quinoline caged acetate **19** was prepared using the same strategy. Considering the relative instability of the tris[4-(ethynylphenyl)]-amine core towards polymerisation, we chose to start from the silylated precursor[9b] **17** and to use slightly modified Sonogashira reaction conditions by adding tetrabutylammonium fluoride in the reaction medium for *in situ* alkyne deprotection. This Sonogashira coupling/deprotection one-pot protocol provided the expected trialdehyde **18** with a satisfactory yield of 47% (corresponding to an average yield of 78% for the three consecutive coupling reactions). Sequential aldehyde reduction with sodium borohydride followed by acetylation with acetic anhydride afforded the targeted octupolar 8-substituted quinoline caged acetate **19** (90%). Once again, the corresponding triol was not isolated due to its lack of solubility in common organic solvents.

In parallel, for comparison purpose, we prepared the quadrupolar analogue of derivative **8** built from a fluorenyl core instead of a triphenylamine core and bearing 6-quinoline uncaging end moieties (compound **21** in Scheme 3). Quadrupolar derivatives built from a fluorenyl core and ethynyl linkers have long been shown to provide an interesting route towards 2PA chromophores combining significant 2PA responses and

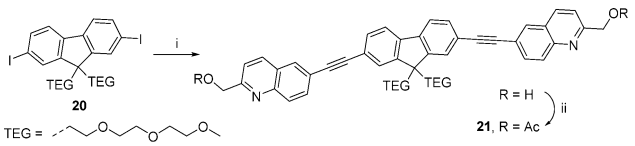

Scheme 3 Reagents and conditions: (i) **3** (2.4 equiv.), $PdCl_2(Ph_3P)_2$ (0.04 equiv.), CuI (0.08 equiv.), THF–Et_3N (20 : 1), RT, overnight, then (ii) *in situ*, DMAP (0.1 equiv.), Ac_2O (2.0 equiv.), RT, overnight, 95%.

transparency.[16] Compound **21** was successfully synthesised in a one pot two-step sequence from the fluorenyl core[17] **20** and 6-ethynylquinoline **3** by Sonogashira cross-coupling followed by the acetylation reaction (Scheme 3).

All new compounds were fully characterised by ^1H, ^{13}C NMR spectroscopy, HRMS. Interestingly, from the splitting values observed for acetylenic carbon in derivatives **8** and **19**, we could obtain an estimation of the Hammett constant values for 6-quinoline and 8-quinoline moieties using the linear relationships previously established for octupolar fluorophores built from a triphenylamine core and ethynyl linkers.[9f] The σ values derived using this methodology are 0.3 and 1.1 for 6-quinoline and 8-quinoline respectively.[18] This suggests that these moieties behave as good acceptors when connected *via* a conjugated linker to a strong electron-donating group, the 8-quinoline showing a stronger electron-withdrawing ability.

Photophysical properties

Absorption and fluorescence properties in organic environments. The photophysical properties of the chimeric and reference compounds were first investigated in aprotic organic solvents (where photolysis is reduced due to lack of water). The experimental data obtained in THF are collected in Table 1. As illustrated in Fig. 3, all compounds display strong absorption in the UV region. The low-energy, broad and intense absorption band in the near UV region (maxima between 368 and 385 nm) is characterised by a high molar extinction coefficient (up to 9.3×10^4 M^{-1} cm^{-1}) which is about one order of magnitude larger than those reported for the DMAQ series.[11] This band is characteristic of an intramolecular charge transfer (ICT) transition, as corroborated by the large Stokes shift values. An additional, narrower, absorption band is observed in the UV region (maxima around 300 nm), which can be ascribed to a higher energy π–π^* transition. As noted from Table 1, all derivatives exhibit significant fluorescence in the visible region, with fluorescence quantum yields ranging from 0.56 to 0.77 in THF.

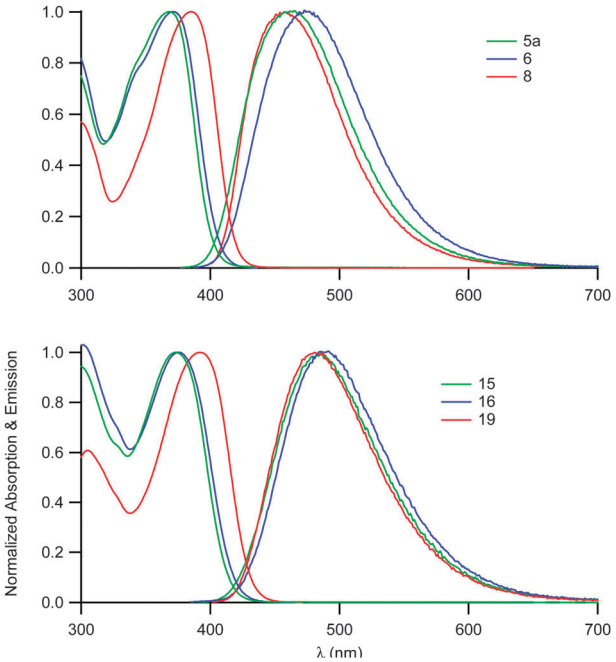

Fig. 3 Absorption and emission spectra of compounds **5a**, **6**, **8** (top) and **15**, **16**, **19** (bottom) in THF.

Table 1 Photophysical properties of the dipolar, quadrupolar and octupolar compounds in THF

	λ_{abs}^{max} [nm]	$\log(\varepsilon^{max})$ [M^{-1} cm^{-1}]	λ_{em}^{max} [nm]	Stokes shift[a] [10^3 cm^{-1}]	Φ_f[b,c]	τ[d] [ns]	k_r[e] [10^9 s^{-1}]	k_{nr}[e] [10^9 s^{-1}]
5a	368	4.58	465	5.7	0.64	2.4	0.27	0.15
	296	4.48						
6	371	4.53	473	5.8	0.65	2.5	0.26	0.14
	296	4.46						
8	385	4.97	457	4.1	0.56	1.7	0.32	0.26
	292	4.73						
13	370	4.46	459	5.2	0.77	2.5	0.30	0.09
	300	4.43						
15	373	4.45	486	6.2	0.60	3.4	0.17	0.12
	300	4.41						
16	376	4.38	488	6.1	0.63	3.6	0.17	0.10
	301	4.39						
19	392	4.85	482	4.8	0.59	2.6	0.22	0.16
	305	4.63						
21	366	4.95	392	1.8	0.68	0.7	0.97	0.47

[a] Stokes shift = $1/\lambda_{abs} - 1/\lambda_{em}$. [b] Φ = fluorescence quantum yields. [c] Standard: quinine (Φ = 0.546) in 0.5 M aq H_2SO_4. [d] Fluorescence lifetime determined using time-correlated single-photon counting. [e] Radiative ($k_r = \Phi/\tau$ and non-radiative $k_{nr} = (1-\Phi)/\tau$) decay rates.

Comparison of the properties of the one-branch (''dipolar'') and three-branch (''octupolar'') derivatives having the same peripheral groups (**6** *versus* **8** and **16** *versus* **19**) confirms that the triphenylamine core mediates electronic coupling between the branches leading to a definite red-shift (15 nm and 16 nm respectively) of the absorption band.[19] In contrast, a blue shift (16 nm and 6 nm respectively) of the emission band is observed. As a result,[20] the radiative decay rates of the octupolar derivatives are increased compared to those of the dipolar ones. This can be interpreted as a consequence of excitation localisation on a dipolar branch prior to emission, leading to a polarised excited state (*vide infra*) whose energy is slightly increased by the proximity of the other dipolar branches, due to destabilising dipole–dipole through-space interactions.[21] In all cases, we also observe a decrease of the fluorescence lifetime which results from the enhancement of the non-radiative decay rate. This is consistent with additional vibrational deactivation modes in the three-branched architectures. Interestingly the larger radiative decay rates almost compensate for the increased

non-radiative decay rates leading to similar fluorescence quantum yields for one-branch (dipolar) and three-branch (octupolar) related derivatives (Table 1).

The position of the donating substituent (4-ethynylphenyl)-diphenylamine on the quinoline moiety is found to influence the photophysical properties of both dipolar (compounds **5a**, **6** *versus* **15**, **16**) and octupolar (compound **8** *versus* **19**) derivatives. A slight red-shift of the absorption spectra (5–7 nm) and a hypochromic effect are observed for derivatives built from 8-quinoline terminal groups compared to their analogues having 6-quinoline terminal groups. Interestingly, an even more pronounced red-shift (15–25 nm) of the emission spectra is observed resulting in larger Stokes shift values. Hence 8-quinoline derivatives show lower energy gaps (E_{00}) in agreement with the estimated stronger electron-withdrawing character. Both radiative rate and non-radiative rates are smaller leading to longer lifetimes but similar fluorescence quantum yields.

Comparing the data obtained for the 8-substituted compounds **13** and **15**, we also observed that the introduction of a polar hydroxyl group on the quinoline side chain induces a bathochromic shift of the absorption spectrum and more strikingly of the emission band (Table 1). The decrease of the fluorescent quantum yield values can be ascribed to combined effects of the reduction of the radiative decay rate (related to the red-shifted emission) and the slight enhancement of the non-radiative decay rate which parallels the increase of the fluorescence lifetime. Further red-shifts of both absorption and emission bands are observed on going from the hydroxyl to the acetyl group. This suggests that the close hydroxyl or acetyl dipoles adopt a relative orientation allowing the stabilisation of the polarised (relaxed) excited state, and thus leads to lower transition energy. We also observe that the fluorescence quantum yield and lifetime values of acetyl derivatives are maintained (compared to their hydroxyl analogues), indicating that no noticeable photochemical processes (*i.e.* uncaging of acetic acid) occur in pure THF. This is consistent with a photorelease mechanism involving water molecules.[11b,d–g]

Finally, it is interesting to note that the reference quadrupolar derivative **21** shows similar absorption properties (low-energy absorption band) as the related dipolar and octupolar derivatives (*i.e.* **6** and **8**) having the same uncaging moieties but markedly blue-shifted emission. The resulting markedly smaller Stokes shift value suggests that the ICT phenomenon leading to symmetry-breaking after excitation and subsequent emission from a localised polarised excited state[22] is not strongly operative in that case.[23] Also both the radiative and non-radiative rates are found to be much larger than those of its dipolar and octupolar counterparts, suggesting larger delocalisation in the excited state and more efficient vibrational deactivation processes.

Solvatochromism. The influence of the environment was investigated by studying the photophysical properties of the chromophores in organic solvents of various polarities (Fig. 4). The absorption spectra are found to be almost unaffected by the change in solvent polarity (except for a high polarity solvent like DMSO which leads to the decrease of the molar extinction coefficients probably due to inhomogeneous broadening). In contrast, increasing the solvent polarity induces a marked bathochromic shift of the emission spectra (responsible for lower radiative decay rates) and subsequently the Stokes shift

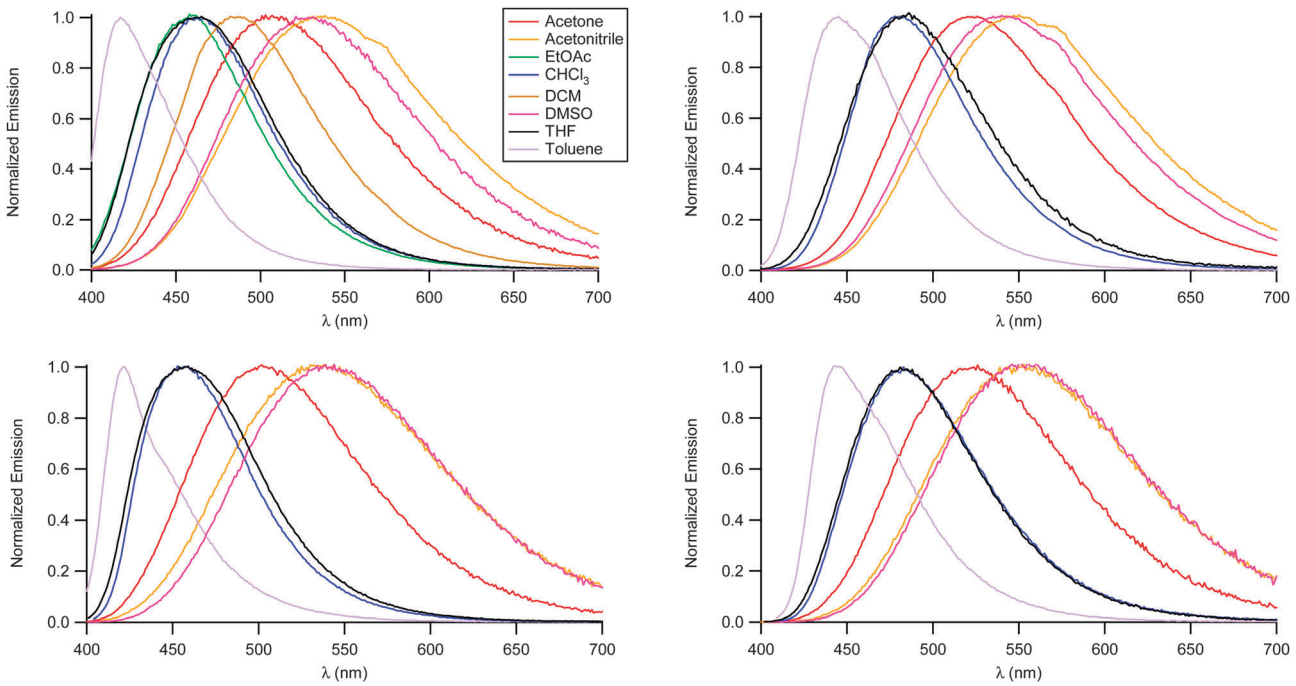

Fig. 4 Solvatochromic behaviour of 6-quinoline derivative compounds **5a** (top left) and **8** (bottom left) and 8-quinoline derivatives **15** (top right) and **19** (bottom right).

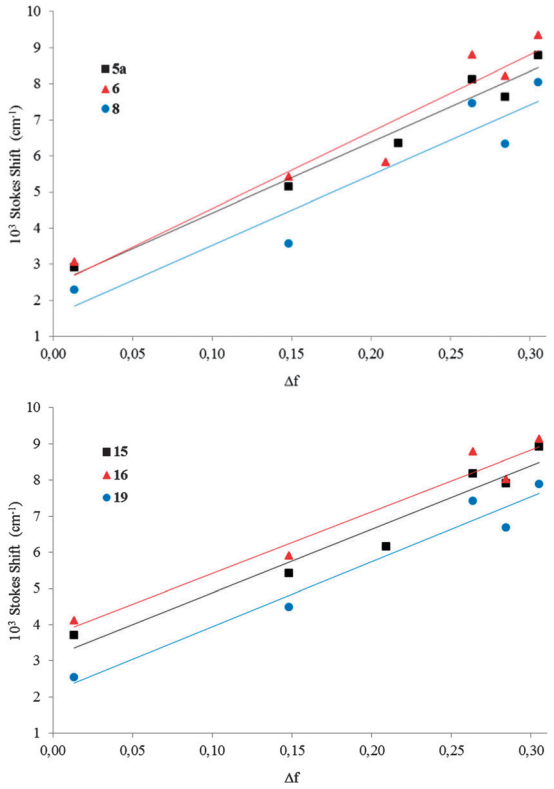

Fig. 5 Lippert–Mataga correlations for compounds **5a**, **6**, **8** (top) and **15**, **16**, **19** (bottom).

increases. Such positive solvatochromic behaviour is consistent with an ICT transition with a large dipole moment enhancement upon excitation. Interestingly both dipolar (compounds **5a**, **6** and **15**, **16**) and related octupolar derivatives (compounds **8** and **19**) did show similar pronounced solvatochromic behaviour. This can be ascribed to excitation localisation, after excitation prior to emission, on the branches of octupolar derivatives leading to polarised emissive states.[9c] In contrast, the symmetrical quadrupolar derivative 21 does not show a marked emission solvatochromism (see ESI†), which suggests that in that case, excitation localisation on part of the molecule does not occur in organic solvents.[24] As shown in Fig. 5, the solvatochromic behavior of dipolar and octupolar compounds can be fitted with a Lippert–Mataga relationship[25] (eqn (1)) as the Stokes shift values are found to depend linearly on the polarity–polarisability (or orientational polarisability) parameter of the solvent Δf:

$$\nu_{abs} - \nu_{em} = 2(\Delta\mu^2/hca^3)\Delta f + \text{const} \qquad (1)$$

where ν_{abs} (ν_{em}) is the wavenumber of the absorption (fluorescence) maximum, h is the Planck constant, c is the light velocity, a is the radius of the Onsager cavity, and $\Delta f = (\varepsilon - 1)/(2\varepsilon + 1) - (n^2 - 1)/(2n^2 + 1)$, where ε is the dielectric constant and n the refractive index of the solvent while $\Delta\mu$ is the change of dipole moment of the solute between ground and excited states. The corresponding slope values derived from the linear variations (*i.e.* $2\Delta\mu^2/hca^3$) are collected in Table 2. Large values are obtained

Table 2 Solvatochromism analysis and anisotropy data of dipolar chimeric derivatives

	Specific solvatochromic shift[a] (10^3 cm^{-1})	r [b]	τ[c] [ns]	θ[d] [ns]	v[e] (Å^3)	a[f] (Å)	$\Delta\mu$[g] (D)
5a	19.7	0.22	3.2	3.9	930	6.1	20.9
6	21.4	0.21	3.2	3.5	842	5.9	20.7
8	19.5	—	—				
15	17.6	0.15	4.7	2.8	670	5.4	16.7
16	17.1	0.15	4.8	2.9	690	5.5	16.7
19	18.0	—	—				

[a] Absolute value of the slope derived from the linear dependency of the Stokes shift on the orientational polarisability ($2\Delta\mu^2/hca^3$). [b] Fluorescence anisotropy in triacetin. [c] Fluorescence lifetime in triacetin. [d] Longitudinal rotational correlation time in triacetin. [e] Molecular volume derived from fluorescence anisotropy. [f] Onsager cavity radius estimated from the molecular volumes. [g] Photo-induced change of dipole moment ($\Delta\mu$).

(from 17.6 to 19.7 × 10^3 cm^{-1}) indicative of a large increase of dipole moment in the excited state for all investigated derivatives. We observe that 6-quinoline derivatives show larger slope values than their corresponding analogue having 8-quinoline moieties. To further derive $\Delta\mu$ values, accurate estimation of the Onsager cavity radius (a) is required. In the case of dipolar derivatives, we conducted anisotropy (r) and fluorescence lifetime measurements (τ) in a viscous solvent in order to gain more information on the size of the molecules and estimate the Onsager cavity radius.[26] Using the Perrin equation[27] (eqn (2)), we calculated the longitudinal rotational correlation time θ from which we derived the effective molecular volume (v) and subsequently estimated the Onsager cavity radius (a):

$$r_{max} = \frac{0.4}{1 + \frac{\tau}{\theta}} \quad \text{with } \theta = \frac{\eta v}{kT} \qquad (2)$$

where η is the solvent viscosity and T the temperature.

The data are collected in Table 2. As expected the caged compound and their precursors (**5a** and **6**, **15** and **16**) show similar $\Delta\mu$ values. In contrast, the 6-quinoline derivatives show larger $\Delta\mu$ values (21 D) than 8-quinoline derivatives (16.5 D). This may sound surprising since the electron-withdrawing ability of the 8-quinoline has been estimated to be somewhat larger. This can however be explained by the shorter distances between the donating and accepting centres in the 8-derivatives compared to the 6-derivatives. Indeed the distance between the donating and accepting nitrogen atoms is 4 Å longer for 6-quinoline derivatives as compared to 8-quinoline analogues.

We also note that related dipolar and octupolar fluorophores (**6** and **8**, **16** and **19**) show similar slope values (Table 2) providing evidence that excitation localisation on the branches occurs prior to emission in octupolar derivatives leading to similarly polarised emissive (relaxed) excited states in octupolar derivatives and related dipolar derivatives.

Two-photon absorption (2PA)

Thanks to their fluorescence properties, we could experimentally determine the 2PA characteristics of all compounds in the

Table 3 Two-photon absorption properties of chimeric quinoline derivatives in THF

	$2\lambda_{abs}^{max}$ [nm]	λ_{TPA}^{max} [nm]	σ_2 at λ_{TPA}^{max} [GM]
5a	736	740	160
6	742	750	163
8	770	730	480
13	740	750	100
15	746	750	130
16	752	750	110
19	784	730	390
21	732	710	75

NIR range (700–900 nm) using the well-known two-photon induced fluorescence (TPEF) technique.[28] Measurements were conducted in THF. Data are collected in Table 3. Interestingly, all multipolar chimeric compounds were found to display much larger (typically between one and two orders of magnitude larger) 2PA cross section values compared to those reported for the most common caging groups[1] and quinoline derivatives.[11h,29]

As observed from Fig. 6, dipolar derivatives **5a**, **6**, **13** and **15** exhibit a broad 2PA band (maxima range: 740–760 nm) occurring at about twice the wavelength of the OPA band, which is consistent with the fact that the lowest-energy excited state is both one and two-photon allowed for dipolar chromophores. We observe that maximum values ranging from 100 to 160 GM are already much larger than those reported for quinoline derivatives.[11h,27] Octupolar chromophores **8** and **19** also present this lowest-energy one- and two-photon allowed absorption band but a major broadening is observed due to the overlap with a more intense 2PA band (maximum at 730–740 nm) located at slightly higher energy and related to the two-photon allowed, one-photon forbidden higher excited state (Fig. 6). As a result the octupolar derivatives show major 2PA enhancement as compared to their dipolar analogues, leading to a 2PA response as high as 480 GM and 390 GM for octupolar derivatives **8** and **19** built from 6-quinoline and 8-quinoline uncaging moieties respectively. The chimeric derivatives built from 6-quinoline derivatives (both dipolar and quadrupolar) always show larger 2PA responses (by 25 to 45%) than their

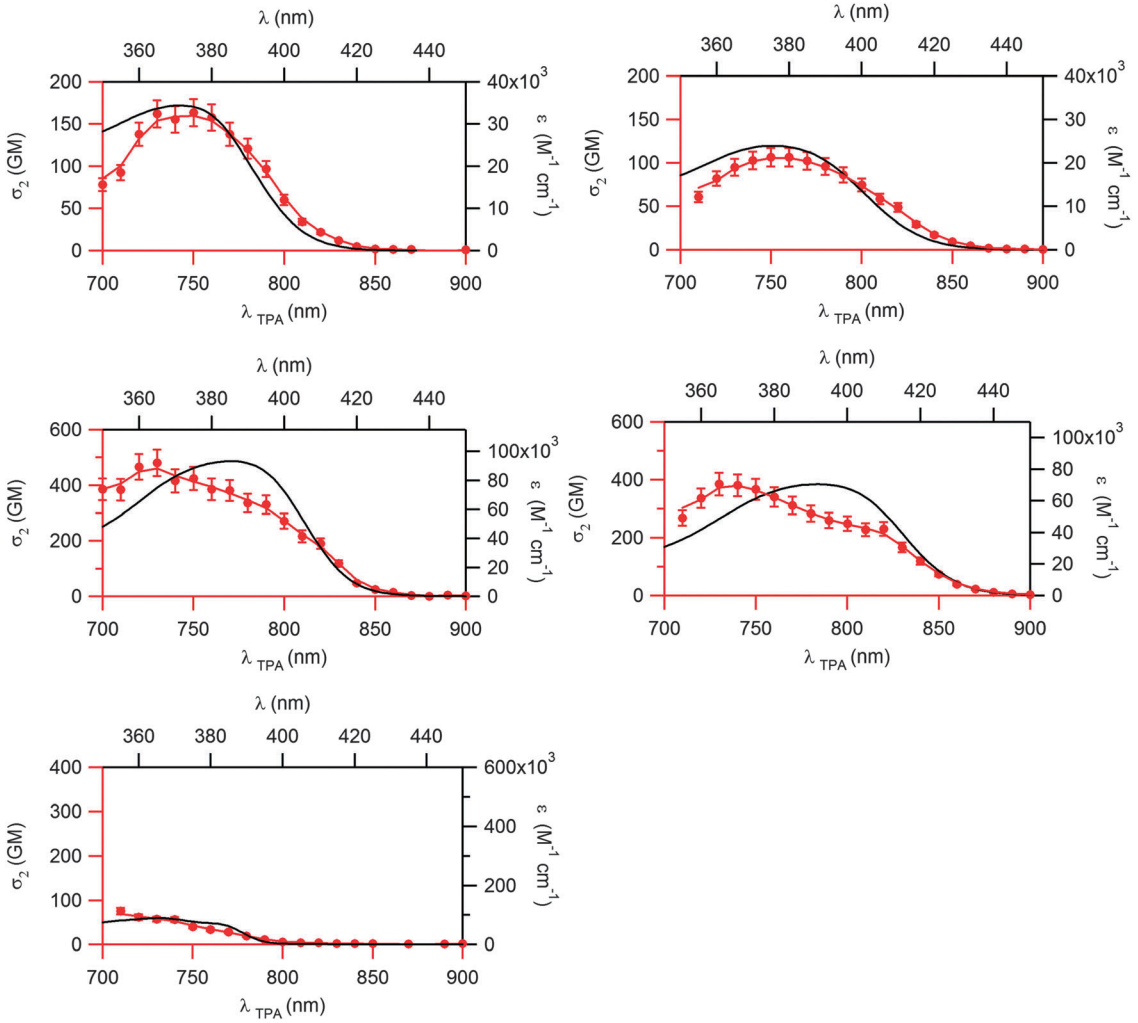

Fig. 6 Compared one-photon absorption (black line) and two-photon absorption (red line) spectra of compounds **6** (top left), **8** (middle left), **21** (bottom left), **16** (top right) and **19** (middle right) in THF.

8-quinoline counterparts (Table 3 and Fig. 6). This parallels the hyperchromic effect observed for one-photon absorption (*vide supra* and Table 1).

In contrast, we observe that the quadrupolar derivatives built from the fluorenyl core show a much smaller 2PA response in the 700–900 nm spectral range (Fig. 6 and Table 3). These lower values can be explained by symmetry reasons as well known for quadrupolar derivatives.[30]

In this case the lowest energy, one-photon allowed, excited state is almost two-photon forbidden leading to low 2PA responses in the NIR range.[16b] The higher excited-state (two-photon allowed, but one-photon forbidden) is most probably located in the visible region. Hence the quinoline derivatives built from a triphenylamine core are more promising chimeric structures than their quadrupolar analogues built from a fluorenyl core in terms of 2P excitation efficiency in the NIR.

Interestingly, we observe that the presence of the hydroxyl appendices leads to a definite increase of the 2PA response of 8-quinoline derivatives as indicated by comparison of the 2PA responses of derivatives **15** and **16**. This confirms that the electric field created by local dipoles close to the chromophore unit can affect the 2PA response in a significant way.[31]

Photo-uncaging studies

We then investigated the uncaging properties of the dipolar and octupolar quinoline caged acetate derivatives in different environments. Samples were excited at 365 nm (using two lamps, 2 × 6 W) and the time courses for the photolysis reactions were monitored either by ^{1}H NMR analysis or by HPLC-MS analysis. The irradiation time for 90% conversion ($t_{90\%}$ in seconds) was deduced from the fit of the kinetic data and the uncaging quantum yield Q_u was then calculated using the following relationship[11a,b,32] (eqn (3)):

$$Q_u = (I \times \varepsilon_{(365nm)} \times 10^3 \times t_{90\%})^{-1} \quad (3)$$

In all experiments, the one-photon photolysis of the **CouOAc** in a pH 7 buffer was used as a reference to determinate the irradiation intensity of the UV lamps (I in einstein cm^{-2} s^{-1}).[32a,33] We also confirmed that the photo-uncagers exhibit very good stability in aqueous solution as no dark hydrolysis was observed after a few days.

We decided to conduct preliminary studies on the photochemical properties of these multipolar 6-substituted quinoline derivatives by directly light inducing the photorelease of acetic acid in NMR samples and monitoring it by ^{1}H NMR analysis. Either acetone-d_6 (for the dipole **6**) or $CDCl_3$ (for the octupole **8**) was used as the solvent depending on the solubility of the caged compounds. As a typical procedure, we dissolved few milligrams of compound in a deuterated solvent (concentration approximately 10^{-3} M) and then the NMR tube was irradiated with two lamps of 365 nm (2 × 6 W) under dark conditions. After several hours of irradiation, a significant signal corresponding to the release of the acetic acid (δCH_3 = 2.10 ppm) appeared and the signal of the acetyl group (δCH_3 = 2.21 ppm)

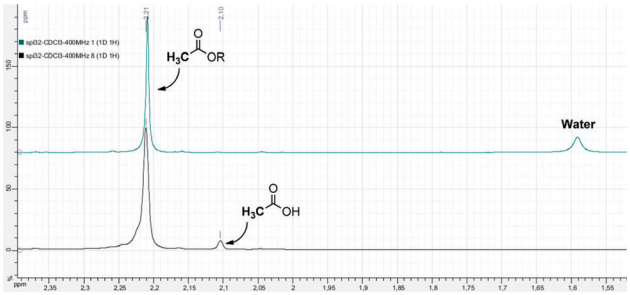

Fig. 7 ^{1}H NMR spectrum (400 MHz) of octupole **8** in $CDCl_3$ at t = 0 h and t = 24 h of irradiation.

of the caged compound simultaneously decreased in both cases (Fig. 7).

This last observation proved that our compounds are able to release the acetyl upon light irradiation. The mechanisms of the photodeprotection reaction of quinoline-based photo-triggers have been investigated in details in recent years.[11b,d–g] It has been highlighted that quinoline caged acetates are classically converted in aqueous media to their respective hydroxyl derivatives upon UV-light excitation and that the photochemical reaction is slower when an organic solvent is used. In these NMR experiments, the formation of the remnant alcohol did not occur due to the lack of water and we observed the formation of a complex mixture which could be explained by the polymerisation of the cationic intermediate species involved in the proposed mechanisms. However the comparison of the integration of the methyl NMR signals allowed us to monitor the time course of the photochemical reaction for the derivative **6** and thus deduce a kinetic profile as well as $t_{90\%}$ and Q_u values (Table 4).

The amount of acetic acid released from the photolysis of the dipolar compound **6** against time fits a single exponential rise to the maximum consistent with a classical photoheterolysis S_N1 reaction mechanism. Estimated values for the uncaging quantum yield (Q_u) and the consequent one-photon uncaging efficiency (εQ_u) are very low in acetone-d_6, pointing to the crucial role of water in the uncaging photochemical process.

We thus turned our attention towards the photolysis of these compounds under simulated physiological conditions using a phosphate buffer titrated to pH 7. As quinoline caged acetate derivatives were not soluble enough in this aqueous medium, experiments were performed in mixtures of phosphate buffer

Table 4 Photochemical properties of chimeric caged acetate compounds

	Solvent	$\varepsilon_{(365nm)}$ (M^{-1} cm^{-1})	Q_u[a]	εQ_u (M^{-1} cm^{-1})
6	Acetone-d_6	3.4×10^4	3.1×10^{-6}	0.10
6	THF–buffer[b] (3 : 7)	4.5×10^4	1.4×10^{-5}	0.65
6	CH_3CN–buffer[b] (1 : 1)	4.1×10^3	1.1×10^{-4}	0.43
8	THF–buffer[b] (1 : 1)	1.1×10^5	7.0×10^{-6}	0.79
16	CH_3CN–buffer[b] (3 : 4)	8×10^3	2.0×10^{-4}	1.6
21	CH_3CN–buffer[b] (1 : 1)	9.5×10^4	1.7×10^{-6}	0.16

[a] Measured at 365 nm. [b] Phosphate buffer adjusted at pH = 7.

with a miscible organic solvent, either acetonitrile (classically used in the literature) or THF depending on the solubility of the phototrigger. Once again, samples were photolysed at 365 nm (using two lamps, 2 × 6 W) and the time courses for the photolysis reactions were monitored this time by HPLC-MS analysis of aliquots taken at periodic intervals. When solutions of dipoles in acetonitrile/phosphate buffer were irradiated, a single new peak was observed in the HPLC chromatogram, which corresponds to the expected remnant alcohols. These identifications were confirmed by comparison with the HPLC-MS analyses under identical conditions to the authentic samples. UV-detection of the elute fractions from the HPLC column was performed either at 254 nm or 365 nm and the two detection modes led to the same results. Analyses of known mixtures of the caged compound and the corresponding alcohol allowed us to plot calibration curves with the classical detection at 254 nm and thus to access quantitative analyses of the time course of the reaction. According to previous observations, the plot of the consumption of the photosensitive dipoles against time fits a simple exponential decay, in agreement with a S_N1 type mechanism. Uncaging quantum yields (Q_u) are much higher than the values observed in organic solvents but still remain very low with typical values of 0.01% and 0.02% for dipolar derivatives having 6-quinoline or 8-quinoline uncaging moieties respectively (*i.e.* compounds **6** or **16**) in a CH_3CN–buffer mixture (Table 4). We also observe that whereas 8-quinoline derivatives show reduced 2PA response compared to 6-quinoline analogues, the uncaging efficiency follows the reverse trend, as reported earlier for DMAQ derivatives.[11h] Interestingly we observe that the quadrupolar derivative **21** shows *a two orders of magnitude smaller uncaging quantum yield* than the dipolar derivative having the same uncaging unit *i.e.* **6** (Table 4).

As the compounds (in particular octupolar derivatives) were found to be more soluble in THF, we conducted the same type of experiments with solutions in a THF–buffer mixture. Under these conditions, the product of the photolysis of the 6-substituted quinoline caged acetate **6** was more complex and HPLC analysis revealed the formation of two different photolysis products with t_R = 20.1 and 26.5 min (Fig. 8). The peak at t_R = 20.1 min with *m*/*z* 427 for MH^+ clearly corresponds to the expected remnant alcohol **5a**. ESI-MS of the second peak corresponding to the retention time 26.5 min showed a signal at *m*/*z* 499 which was attributed to the MH^+ response of the alcohol **5b** (Scheme 4). It appeared that THF could play the role of a competitive nucleophile during the photochemical process. Trapping of the carbocationic intermediate might occur through the ring opening of the THF molecule prior to the water addition, leading to the alcohol **5b** (Scheme 4). The product outcome of the photolysis of the corresponding octupoles under different solvent conditions and the associated kinetic profiles are even more complex. The photochemical reaction classically induces the release of acetic acid and produces at least three other products corresponding to the mono-, bis- and tris-deprotected molecules when non nucleophilic solvents are used (for example acetonitrile).

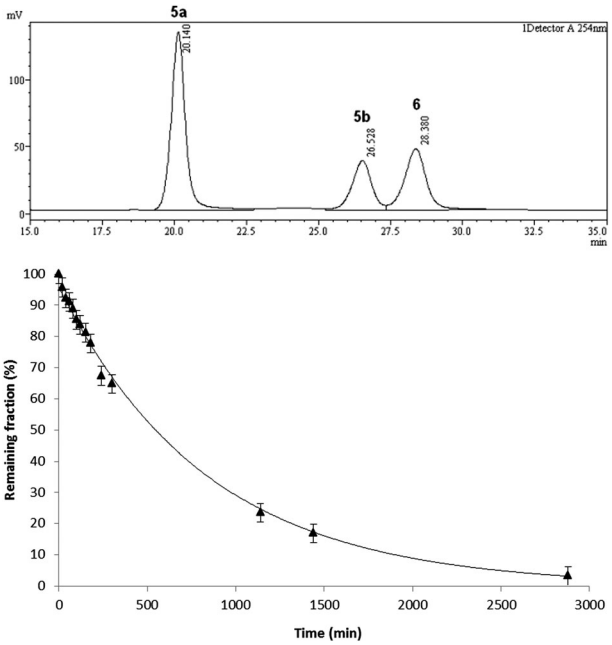

Fig. 8 The one-photon photolysis at 365 nm of the 6-substituted quinoline dipole **6** performed in a THF–buffer pH 7 mixture (1.1×10^{-4} M): (top) HPLC chromatogram obtained after irradiation of the sample; (bottom) plot of the remaining fraction of the photoactive compound against time. The solid line is a least-squares fit of a simple decaying exponential (coefficient of determination R^2 = 0.99).

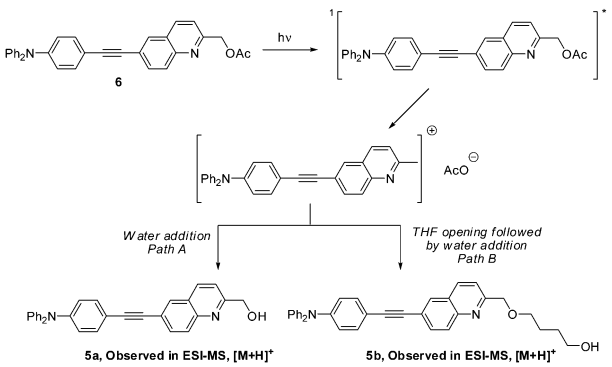

Scheme 4 Proposed reaction routes of compound **6** in a THF–water mixture.

Considering the nucleophilicity of the THF, we could now expect the formation of nine remnant alcohols from the photolysis of the octupolar 6-substituted quinoline caged acetate **8** in a 1/1 THF–buffer pH 7 mixture. After optimisation of the elution conditions, HPLC analysis of the irradiated sample revealed six well separated peaks with retention times of 20.0, 23.7, 25.0, 29.3, 31.1 and 33.2 min. The correspondence between them and the different by-products was clearly established thanks to the ESI-MS analysis of the elute corresponding to each peak showing signals for MH^+ at *m*/*z* 789, 861, 831, 933, 903 and 873, respectively. The search in the chromatogram for specific MH^+ signals allowed us to confirm that the three other remnant alcohols were not produced in sufficient amounts to be detected by the UV sensor. Reasonably assuming that all the

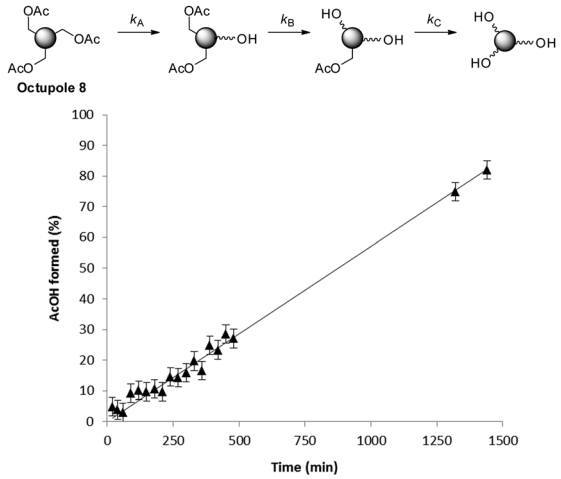

Fig. 9 Time course of one-photon photolysis of octupole **8** at 365 nm. Relative concentrations of remnant alcohols were determined by HPLC. The deduced relative amount of acetic acid released against time is plotted. The solid line is a least-squares fit of a linear rise (coefficient of determination $R^2 = 0.99$).

six identified remnant alcohols display similar absorption properties at 365 nm, we could calculate the relative amount of released acetate in the different aliquots from the integration of the HPLC peaks. 90% of acetate release was achieved after 1 day of irradiation. The production of acetic acid against time is plotted in Fig. 9 and the apparent kinetics seems to fit a linear profile.

As reported in Table 4 for the dipolar derivative **6**, the uncaging efficiency is observed to be reduced by almost one order of magnitude in the THF–buffer mixture as compared to the CH_3CN–buffer mixture. This emphasises that the polarity of the environment as well as the amount of water significantly influence and improve the uncaging efficiency. In that respect the lower uncaging yield of the octupolar derivative **8** with respect to its dipolar analogue **6** (by a factor of about 2) could also be related to the larger amount of THF (and subsequent lower amount of water) necessary to dissolve the octupolar derivatives.

The uncaging study thus reveals that the functionalisation of the quinoline cage with an ethynylphenylamine moiety (either in the 6- or 8-position) dramatically affects its ability to undergo photolysis both for dipolar and octupolar derivatives. Using the hypothesis that one- and two-photon uncaging quantum yields are the same (*i.e.* originate from the same lowest excited state and follow the Kasha rule), we could derive two-photon uncaging action cross-sections (δ_u) from the experimentally determined σ_2 values and using the uncaging values (Q_u) measured in CH_3CN–water mixtures. For dipolar derivatives **6** and **16**, maximum δ_u values of about 0.002 GM are obtained at 750 nm. Concerning octupolar derivatives, using an estimated minored value of the uncaging quantum yield (*i.e.* half of that of the dipolar analogue, as derived from comparison of compounds **6** and **8** in Table 4) δ_u values of 0.03 GM and 0.04 GM at 730 nm are estimated for octupolar derivatives **8** and **19** respectively. These values, although modest, are one order of magnitude larger than those obtained for dipolar derivatives demonstrating that octupolar derivatives are more favourable for 2P uncaging than their quadrupolar counterparts.

Conclusion

The present study conducted on a series of multipolar (dipolar, quadrupolar and octupolar) chimeric derivatives of 6- and 8-quinoline demonstrates that the chimeric strategy is indeed promising in terms of enhancing (by up to two orders of magnitude) the two-photon absorption response in the NIR region. Interestingly, the octupolar derivatives show larger two-photon absorption responses than their dipolar analogues whereas the quadrupolar derivative (built from a fluorenyl core instead of having triphenylamine electron-donating moieties as dipolar and octupolar derivatives) shows the smallest two-photon absorption response in the NIR region. However, the chimeric derivatives show much lower uncaging quantum yields than DMAQ-OAc derivatives optimised for one-photon uncaging.[11] The more pronounced – and dramatic – reduction is observed for the quadrupolar derivative built from a fluorenyl core. In contrast, the octupolar derivatives are found to display one-order larger two-photon uncaging cross sections (δ_u) than their dipolar counterparts. This opens an interesting route towards an optimised ''octupolar type structure'' where two-photon absorption enhancement offered by the octupolar scheme would be combined with satisfactory uncaging efficiency. The uncaging quantum yields of quinoline derivatives have been shown to be fairly dependent on the nature (and position) of substituents.[11] We are thus currently exploring other quinoline moieties, as well as alternative uncaging moieties in order to further engineer octupolar chimeric structures where uncaging efficiency would be better retained while taking advantage of the net two-photon absorption enhancement provided by the current octupolar scheme in the spectral range of interest for biological applications (700–1000 nm).

Experimental section

Synthetic procedures

General methods. Melting points were measured on a Stuart SMP 10. Infrared spectra were measured on a Perkin Elmer Spectrum 100 Optica. ^1H and ^{13}C NMR spectra were recorded on a Bruker Avance III 200 spectrometer at 200 MHz and 50 MHz respectively and on a Bruker Avance I 300 spectrometer at 300 MHz and 75 MHz, respectively. Shifts (δ) are given in parts per million with respect to the solvent residual peak and coupling constants (J) are given in Hertz. Mass spectra were performed by the CESAMO (Bordeaux, France) on a QStar Elite mass spectrometer equipped with an ESI source. Elemental Analyses were carried out by the ''Institut de Chimie des Substances Naturelles'' (Gif-sur-Yvette, France). LC/MS analyses were performed on a Shimadzu LCMS-2020. Column chromatography was performed on Fluka silica gel 60 (40–63 μm). Solvents were freshly distilled before being used over CaH_2

(for toluene, CH_2Cl_2 and Et_3N) or benzophenone–Na (for THF). $CDCl_3$ was neutralised with K_2CO_3 prior to use. No melting point value is indicated when compounds decomposed.

(6-Bromoquinolin-2-yl)methanol (2)[12]. A suspension of selenium oxide (1.33 g, 12 mmol) in dry dioxane (50 mL) was heated for 1 h at 60 °C, and then 6-bromo-2-methylquinoline (2.23 g, 10 mmol) was added in one portion. The resulting red mixture was heated at reflux for 3 h. After cooling to room temperature, the mixture was filtrated through celite, the solid part was washed with dioxane and the filtrate was concentrated under reduced pressure. The resulting yellow solid was dissolved in methanol (100 mL), cooled to 0 °C, and sodium borohydride (760 mg, 20 mmol) was added. The resulting mixture was stirred overnight at room temperature, and then concentrated under reduced pressure. The residue was neutralised with water and extracted with CH_2Cl_2. The combined organic layer was dried (Na_2SO_4) and then concentrated under reduced pressure. A short column of silica gel (eluent, CH_2Cl_2 : EtOAc 8 : 2) gave compound **2** (2.05 g, 86%) as a white powder. ^{1}H NMR (DMSO-d_6, 200 MHz) δ (ppm): 8.35 (d, J = 8.7 Hz, 1H), 8.25 (d, J = 1.8 Hz, 1H), 7.80 (m, 2H), 7.70 (d, J = 8.5 Hz, 1H), 5.59 (t, J = 6.0 Hz, 1H, OH), 4.72 (d, J = 6.0 Hz, 2H).

(6-Ethynylquinolin-2-yl)-methanol (3). Argon was bubbled into a mixture of (6-bromoquinolin-2-yl)methanol **2** (730 mg, 3.06 mmol), in a dry mixture of toluene–Et_3N (30 mL, 5 : 1) for 20 min. Then, copper iodide (29.2 mg, 0.15 mmol), $PdCl_2(Ph_3P)_2$ (107.4 mg, 0.153 mmol), Ph_3P (160 mg, 0.612 mmol), and ethynyltrimethylsilane (640 μL, 4.5 mmol) were added. The resulting mixture was heated at 60 °C for 16 h. The mixture was cooled at 0 °C and TBAF (1M in THF, 6 mL, 6 mmol) was added. The reaction mixture was stirred for 1 h at room temperature, and filtrated through celite. The filtrate was concentrated under reduced pressure. The residue was diluted in EtOAc, and washed with water. The combined organic layer was washed with brine, dried (Na_2SO_4), and concentrated under reduced pressure. The crude product was purified on silica gel (eluent, CH_2Cl_2 : EtOAc 9 : 1) to give compound **3** (440 mg, 79%) as an orange powder. Mp 129 °C. IR (KBr) ν (cm^{-1}): 3333, 3264, 3213, 1592, 1494, 1071, 1043, 883, 833. ^{1}H NMR (DMSO-d_6, 200 MHz) δ (ppm): 8.37 (d, J = 8.5 Hz, 1H), 8.16 (d, J = 1.7 Hz, 1H), 7.93 (d, J = 8.7 Hz, 1H), 7.74 (dd, J = 8.7 Hz, J = 1.7 Hz, 1H), 7.70 (d, J = 8.5 Hz, 1H), 5.59 (t, J = 6.0 Hz, 1H, OH), 4.72 (d, J = 6.0 Hz, 2H), 4.33 (s, 1H). ^{13}C NMR (DMSO-d_6, 75 MHz) δ (ppm): 64.7, 81.6, 83.2, 119.1, 119.8, 126.6, 128.8, 131.8, 131.9, 136.3, 146.2, 163.7. ESIHRMS: $C_{12}H_9NO$ calculated for $[M + Na]^+$: 206.0576, found 206.0567. Anal. calcd for $C_{12}H_9NO$: C, 77.90; H, 5.01; N, 7.57; found: C, 78.10; H, 4.84; N, 7.30.

(6-[(4-(Diphenylamino)phenyl)ethynyl]quinolin-2-yl)-methanol (5a). Argon was bubbled into a solution of (4-iodophenyl)diphenylamine **4** (200 mg, 0.53 mmol) and (6-ethynylquinolin-2-yl)-methanol **3** (118 mg, 0.65 mmol), in a dry mixture of THF–Et_3N (6 mL, 5 : 1) for 20 min. Then, copper iodide (12.1 mg, 63.6 μmol) and $PdCl_2(Ph_3P)_2$ (22.3 mg, 31.8 μmol) were added. The resulting mixture was stirred for 2 h at room temperature. The mixture was filtrated through celite. The filtrate was washed with brine and extracted with EtOAc. The combined organic layer was dried (Na_2SO_4), and concentrated under reduced pressure. The crude product was purified on silica gel (gradient eluent, toluene : EtOAc 9 : 1 to 4 : 1) to give compound **5a** (190 mg 84%) as a yellow powder. Mp 172 °C. IR (KBr) ν (cm^{-1}): 3434, 3061, 3034, 2199, 1589, 1509, 1334, 1315, 1285, 1268, 1062, 834, 754, 696. ^{1}H NMR ($CDCl_3$, 300 MHz) δ (ppm): 8.08 (d, J = 8.5 Hz, 1H), 8.02 (d, J = 8.7 Hz, 1H), 7.99 (d, J = 1.7 Hz, 1H), 7.81 (dd, J = 8.7 Hz, J = 1.7 Hz, 1H), 7.43 (d, J = 6.7 Hz, 2H), 7.26–7.33 (m, 5H), 7.01–7.16 (m, 8H), 4.93 (s, 2H). ^{13}C NMR ($CDCl_3$, 75 MHz) δ (ppm): 64.4, 88.4, 91.3, 115.8, 119.2, 122.0, 122.3, 123.9, 125.3, 127.6, 128.9, 129.6, 130.8, 132.8, 136.6, 146.3, 147.3, 148.4, 159.7. ESIHRMS: $C_{30}H_{22}N_2O$ calculated for $[M + Na]^+$: 449.1624, found 449.1609. Anal. calcd for $C_{30}H_{22}N_2O$: C, 81.72; H, 5.39; N, 6.35; found: C, 81.96; H, 5.15; N, 5.98.

(6-[(4-(Diphenylamino)phenyl)ethynyl]quinolin-2-yl)-methyl acetate (6). To a solution of (6-[(4-(diphenylamino)phenyl)-ethynyl]quinolin-2-yl)-methanol **5a** (100 mg, 0.23 mmol), DMAP (2.8 mg, 23 μmol), and Et_3N (62.2 μL, 0.46 mmol) in dry CH_2Cl_2 (3 mL) Ac_2O (44 μL, 0.46 mmol) was added. The yellow solution was stirred for 4 h at room temperature, quenched with an aqueous saturated $NaHCO_3$ solution, and then extracted with CH_2Cl_2. The combined organic layer was dried (Na_2SO_4), and concentrated under reduced pressure. The crude product was purified on silica gel (eluent, heptane : EtOAc 4 : 1) to give compound **6** (106 mg, 99%) as a brown powder. Mp 146 °C. IR (KBr) ν (cm^{-1}): 3056, 3036, 2926, 1739, 1590, 1507, 1492, 1329, 1314, 1245, 1228, 1059, 834, 752, 694, 501. ^{1}H NMR ($CDCl_3$, 300 MHz) δ (ppm): 8.06 (d, J = 8.5 Hz, 1H), 7.95 (d, J = 8.7 Hz, 1H), 7.90 (d, J = 1.7 Hz, 1H), 7.72 (dd, J = 8.7 Hz, J = 1.7 Hz, 1H), 7.40 (d, J = 8.5 Hz, 2H), 7.33 (d, J = 8.7 Hz, 1H), 7.17–7.25 (m, 4H), 6.92–7.07 (m, 8H), 5.31 (s, 2H), 2.13 (s, 3H). ^{13}C NMR ($CDCl_3$, 75 MHz) δ (ppm): 21.1, 67.6, 88.4, 91.5, 115.7, 120.3, 122.3, 122.4, 123.9, 125.3, 127.6, 129.5, 129.7, 129.8, 130.7, 132.8, 132.9, 136.8, 147.1, 147.3, 156.8, 170.9. ESIHRMS: $C_{32}H_{24}N_2O_2$ calculated for $[M + Na]^+$: 491.1729, found 491.1712. Anal. calcd for $C_{32}H_{24}N_2O_2$ C, 81.40; H, 5.21; N, 5.93; found: C, 81.41; H, 5.17; N, 5.84.

(6,6′,6″-[(Nitrilotris(benzene-4,1-diyl))tris(ethyne-2,1-diyl)]-tris(quinolone-6,2-diyl))-tris(methylene) triacetate (8). Argon was bubbled into a solution of tris(4-iodophenyl)amine **7** (131 mg, 0.21 mmol) and (6-ethynylquinolin-2-yl)-methanol **3** (140 mg, 0.76 mmol), in a dry mixture of THF–Et_3N (2.4 mL, 5 : 1) for 20 min. Then, copper iodide (4.8 mg, 25.2 μmol) and $PdCl_2(Ph_3P)_2$ (8.84 mg, 12.6 μmol) were added. The resulting mixture was stirred for 2 h at room temperature. The mixture was diluted with THF (1 mL) and then DMAP (2.6 mg, 21 μmol), and Ac_2O (120 μL, 1.26 mmol) were added. The resulting mixture was stirred overnight at room temperature. The reaction was filtrated through Celite®. The filtrate was diluted with EtOAc, and washed with an aqueous saturated $NaHCO_3$ solution. The organic layer was dried (Na_2SO_4), and concentrated under reduced pressure. The crude product was purified on silica gel (eluent, CH_2Cl_2 : EtOAc 7 : 3) to give compound **8** (180 mg, 94%) as a yellow powder. Mp 112 °C. IR (KBr) ν (cm^{-1}): 3037, 2939, 2204, 1931, 1744, 1591, 1563, 1505, 1477, 1369, 1319, 1224, 1179, 1050, 888, 834, 744, 538. ^{1}H NMR ($CDCl_3$, 300 MHz)

δ (ppm): 8.13 (d, J = 8.5 Hz, 3H), 8.05 (d, J = 8.9 Hz, 3H), 8.00 (d, J = 1.9 Hz, 3H), 7.81 (dd, J = 8.9 Hz, J = 1.9 Hz, 3H), 7.46–7.52 (m, 9H), 7.12 (d, J = 8.7 Hz, 6H), 5.39 (s, 6H), 2.21 (s, 9H). ^{13}C NMR ($CDCl_3$, 75 MHz) δ (ppm): 20.9, 67.4, 89.0, 90.7, 117.8, 120.2, 121.9, 124.2, 127.3, 129.4, 130.7, 132.5, 133.0, 136.6, 146.9, 147.1, 156.8, 170.7. ESIHRMS: $C_{60}H_{42}N_4O_6$ calculated for $[M + Na]^+$: 937.2996, found 937.2999. Anal. calcd for $C_{60}H_{42}N_4O_6$: C, 77.24; H, 4.75; N, 6.00; found: C, 77.10; H, 4.49; N, 5.95.

8-Iodo-2-methylquinoline (10). To a cooled (−70 °C) solution of 8-bromo-2-methylquinoline **9** (2.36 g, 10 mmol), in dry THF (75 mL), was added slowly a solution of *n*-BuLi (2.5 M in hexanes, 4.4 mL, 11 mmol). The resulting brown solution was stirred for 1 h at −70 °C, and then, a solution of iodine (in 25 mL of dry THF) was slowly added. The reaction was warmed slowly at room temperature, and stirred for 1 h at this temperature. The red mixture was quenched with an aqueous $Na_2S_2O_3$ solution. After neutralisation of excess of iodine (red to yellow solution), the aqueous layer was extracted several times with Et_2O. The combined organic layer was dried (Na_2SO_4), and concentrated under reduced pressure. The crude product was purified on silica gel (eluent, Et_2O : petroleum ether, 5 : 95) to give 8-iodo-2-methylquinoline **10** (2.60 g, 97%) as a yellowish powder. Mp: 65 °C. ^{1}H NMR ($CDCl_3$, 400 MHz) δ (ppm): 8.30 (dd, J = 7.4 Hz, J = 1.3 Hz, 1H), 7.95 (d, J = 8.4 Hz, 1H), 7.76 (dd, J = 8.0 Hz, J = 1.3 Hz, 1H), 7.76 (dd, J = 8.0 Hz, J = 1.3 Hz, 1H), 7.31 (d, J = 8.4 Hz, 1H), 7.19 (dd, J = 8.0 Hz, J = 7.4 Hz, 1H), 2.81 (s, 3H). ^{13}C NMR ($CDCl_3$, 100 MHz) δ (ppm): 25.7, 103.4, 123.0, 126.9, 127.1, 128.6, 136.8, 140.0, 146.7, 160.8. ESIHRMS: $C_{10}H_8IN$ calculated for $[M+H]^+$: 269.9774, found 269.9767. Anal. calcd for $C_{10}H_8IN$: C, 44.64; H, 3.00; N, 5.21; found: C, 44.48; H, 3.01; N, 5.54.

8-Iodoquinoline-2-carbaldehyde (11). A mixture of 8-iodo-2-methylquinoline **10** (430 mg, 1.60 mmol) and selenium oxide (215 mg, 1.92 mmol) in 1,4-dioxane (10 mL) was heated at 80 °C for 6 h. The mixture was cooled to room temperature, filtrated through celite, and the filtrate was concentrated under reduced pressure. The crude product was purified on silica gel (eluent, Et_2O : petroleum ether, 1 : 9) to give 8-iodoquinoline-2-carboxaldehyde **11** (410 mg, 91%) as a yellow powder. 165 °C ^{1}H NMR ($CDCl_3$, 600 MHz) δ (ppm): 10.31 (s, 1H), 8.45 (d, J = 7.3 Hz, 1H), 8.25 (d, J = 8.3 Hz, 1H), 8.06 (d, J = 8.0 Hz, 1H), 7.40 (dd, J = 8.0 Hz, J = 7.3 Hz, 1H). ^{13}C NMR ($CDCl_3$, 150 MHz) δ (ppm): 104.9, 118.3, 128.8, 130.3, 130.9, 138.4, 141.3, 146.9, 153.5, 193.5. ESIHRMS: $C_{10}H_6INO$ calculated for $[M + Na]^+$: 305.9386, found 305.9392.

4-((2-Methylquinolin-8-yl)ethynyl)-*N*,*N*-diphenylaniline (13). To a solution of (4-ethynylphenyl)diphenylamine **12** (60.0 mg, 222.7 mol), 8-iodo-2-methylquinoline **10** (53.6 mg, 200.0 μmol), $Pd_2(dba)_3$ (9.2 mg, 10.0 μmol), CuI (3.8 mg, 20 μmol), and Ph_3P (10.5 mg, 40 μmol) in a dry THF (2 mL) was added 100 μL of dry Et_3N. The resulting mixture was stirred for 3 h at room temperature. The reaction was filtrated through a patch of silica gel, washed with Et_2O, and the filtrate was concentrated under reduced pressure. The crude product was purified on silica gel (eluent, toluene), to give 4-((2-methylquinolin-8-yl)ethynyl)-*N*,*N*-diphenylaniline **13** (9.8 mg, 12%) as a brown powder. Mp: 125 °C. ^{1}H NMR ($CDCl_3$, 400 MHz) δ (ppm): 8.34 (d, J = 8.3 Hz, 1H), 7.93 (dd, J = 7.2 Hz, J = 1.4 Hz, 1H), 7.73 (dd, J = 8.0 Hz, J = 1.1 Hz, 1H), 7.54 (d, J = 8.8 Hz, 2H), 7.42–7.47 (m, 1H), 7.27–7.34 (m, 5H), 7.11–7.16 (m, 4H), 7.02–7.09 (m, 4H), 2.82 (s, 3H). ^{13}C NMR ($CDCl_3$, 100 MHz) δ (ppm): 26.0, 87.0, 95.7, 116.8, 122.4, 122.6, 123.1, 123.6, 125.1, 125.3, 126.7, 127.9, 133.0, 133.7, 136.5, 147.4, 148.0, 160.1. ESIHRMS: $C_{30}H_{22}N_2$ calculated for $[M + H]^+$: 411.1855, found 411.1850.

8-((4-(Diphenylamino)phenyl)ethynyl)quinoline-2-carbaldehyde (14). To a solution of (4-ethynylphenyl)diphenylamine **12** (105.0 mg, 338.0 μmol), 8-iodoquinoline-2-carboxaldehyde (100.0 mg, 350.0 μmol), $Pd_2(dba)_3$ (16.0 mg, 17.0 μmol), CuI (6.7 mg, 35.0 μmol), and Ph_3P (18.4 mg, 70.0 μmol) in a dry THF (3 mL) was added 150 μL of dry Et_3N. The resulting mixture was stirred overnight at room temperature. The reaction was filtrated through a patch of silica gel, and the filtrate was concentrated under reduced pressure. The crude product was purified on silica gel (eluent, toluene), to give 8-((4-(diphenylamino)phenyl)ethynyl)-quinoline-2-carbaldehyde **14** (76 mg, 51%) as a yellow powder. Mp: 151 °C. ^{1}H NMR ($CDCl_3$, 400 MHz) δ (ppm): 10.32 (s, 1H), 8.32 (d, J = 8.4 Hz, 1H), 8.07 (d, J = 8.4 Hz, 1H), 8.04 (d, J = 7.2 Hz, 1H), 7.82 (d, J = 8.1 Hz, 1H), 7.65 (dd, J = 8.1 Hz, J = 7.2 Hz, 1H), 7.56 (d, J = 8.6 Hz, 2H), 7.27–7.33 (m, 4H), 7.12–7.17 (m, 4H), 7.04–7.11 (m, 4H). ^{13}C NMR ($CDCl_3$, 100 MHz) δ (ppm): 86.0, 97.6, 115.9, 117.9, 122.2, 123.8, 125.3, 127.8, 128.9, 129.6, 130.3, 133.1, 134.4, 137.9, 147.2, 147.8, 148.5, 152.7, 194.1. ESIHRMS: $C_{30}H_{20}N_2O$ calculated for $[M]^+$: 424.1576, found 424.1581. Anal. calcd for $C_{30}H_{20}N_2O$: C, 84.88; H, 4.75; N, 6.00; found: C, 84.83; H, 4.74; N, 6.23.

8,8′,8″-((Nitrilotris(benzene-4,1-diyl))tris(ethyne-2,1-diyl))-tris(quinoline-2-carbaldehyde) (18). To a solution of tris[4-(2-trimethylsilylethynyl)phenyl]amine[9b] **17** (117.5 mg, 220 μmol), 8-iodoquinoline-2-carboxaldehyde (200 mg, 729.5 μmol), $Pd_2(dba)_3$ (10 mg, 11 μmol), CuI (4.2 mg, 22 μmol), and Ph_3P (11.6 mg, 44 μmol) in a dry mixture of THF–Et_3N (5 : 1, 2.4 mL) was added a solution of TBAF (1 M in THF, 780 μL, 780 μmol). The resulting mixture was stirred overnight at room temperature. The reaction was quenched with an aqueous saturated NH_4Cl solution, and then extracted several times with EtOAc. The combined organic layer was dried and concentrated under reduced pressure. The crude product was purified on silica gel (eluent, Et_2O : CH_2Cl_2, 5 : 95), and the resulting brown powder was washed with pentane to give 8,8′,8″-((nitrilotris(benzene-4,1-diyl))tris(ethyne-2,1-diyl))-tris(quinoline-2-carbaldehyde) **18** (80 mg, 47%) as an orange powder. ^{1}H NMR ($CDCl_3$, 600 MHz) δ (ppm): 10.34 (s, 3H), 8.34 (d, J = 8.4 Hz, 3H), 8.05–8.11 (m, 6H), 7.88 (dd, J = 8.1 Hz, J = 0.6 Hz, 3H), 7.63–7.71 (m, 9H), 7.16–7.22 (m, 6H). ^{13}C NMR ($CDCl_3$, 150 MHz) δ (ppm): 86.8, 97.0, 118.0, 118.2, 124.3, 125.0, 128.1, 128.9, 130.4, 133.4, 134.6, 138.0, 147.2, 147.8, 152.8, 194.1. ESIHRMS: $C_{54}H_{30}N_4O_3$ calculated for $[M + Na]^+$: 805.2210, found 805.2223.

(8-[(4-(Diphenylamino)phenyl)ethynyl]quinolin-2-yl)-methanol (15). To a solution of 8-((4-(diphenylamino)phenyl)ethynyl)quinoline-2-carbaldehyde **14** (44 mg, 103 μmol), in dry THF (1 mL) was added $NaBH_4$ (3.8 mg, 103 μmol). The reaction mixture was stirred overnight at room temperature, quenched with an aqueous

saturated $NaHCO_3$ solution and then extracted several times with CH_2Cl_2. The combined organic layer was dried (Na_2SO_4) and then concentrated under reduced pressure. The crude product was purified on silica gel (20% EtOAc in Petroleum Ether) to give (5-[(4-(diphenylamino)phenyl)ethynyl]quinolin-2-yl)-methanol **15** (35 mg, 82%) as a yellow powder. Mp: 147 °C. ^{1}H NMR ($CDCl_3$, 400 MHz) δ (ppm): 8.16 (d, J = 8.5 Hz, 1H), 7.95 (dd, J = 7.3 Hz, J = 0.9 Hz, 1H), 7.79 (dd, J = 8.0 Hz, J = 1.0 Hz, 1H), 7.47–7.55 (m, 3H), 7.27–7.32 (m, 5H), 7.14 (d, J = 7.7 Hz, 4H), 7.02–7.09 (m, 4H), 4.96 (s, 2H). ^{13}C NMR ($CDCl_3$, 50 MHz) δ (ppm): 64.0, 86.1, 96.3, 116.4, 118.9, 122.5, 123.7, 125.2, 126.2, 127.8, 129.5, 132.9, 133.6, 137.4, 147.3, 148.2, 159.3. ESIHRMS: $C_{30}H_{22}N_2O$ calculated for $[M + Na]^+$: 426.1732, found 426.1728. Anal. calcd for $C_{30}H_{22}N_2O$: C, 84.48; H, 5.20; N, 6.57; found: C, 84.24; H, 5.29; N, 6.55.

(8-((4-(Diphenylamino)phenyl)ethynyl)quinolin-2-yl)methyl acetate (16). To a solution of 8-((4-(diphenylamino)phenyl)-ethynyl)quinoline-2-carbaldehyde **14** (50 mg, 117.8 μmol), in dry THF (4 mL) was added $NaBH_4$ (4.9 mg, 129.6 μmol). The reaction mixture was stirred overnight at room temperature. Then, DMAP (1.4 mg, 11.8 μmol) was added followed by addition of a Ac_2O–Et_3N mixture (1 : 1, 1 mL). The reaction was stirred overnight at room temperature, quenched with an aqueous saturated $NaHCO_3$ solution and then extracted several times with CH_2Cl_2. The combined organic layer was dried (Na_2SO_4) and then concentrated under reduced pressure. The crude product was purified on silica gel (20% EtOAc in Petroleum Ether) to give (8-((4-(diphenylamino)phenyl)ethynyl)quinolin-2-yl)methyl acetate **16** (40 mg, 75%) as a yellow powder. Mp: 156 °C. ^{1}H NMR ($CDCl_3$, 400 MHz) δ (ppm): 8.17 (d, J = 8.4 Hz, 1H), 7.95 (dd, J = 7.1 Hz, J = 1.3 Hz, 1H), 7.77 (dd, J = 8.5 Hz, J = 1.3 Hz, 1H), 7.48–7.54 (m, 4H), 7.27–7.32 (m, 4H), 7.12–7.16 (m, 4H), 7.03–7.09 (m, 4H), 5.49 (s, 2H), 2.21 (s, 3H). ^{13}C NMR ($CDCl_3$, 100 MHz) δ (ppm): 21.1, 67.6, 86.6, 96.1, 116.6, 119.7, 122.4, 123.7, 123.8, 125.2, 126.3, 127.7, 127.8, 129.5, 133.0, 133.9, 137.3, 147.4, 147.5, 148.1, 156.9, 170.9. ESIHRMS: $C_{32}H_{24}N_2O_2$ calculated for $[M + Na]^+$: 491.1729, found 491.1709.

(8,8′,8″-((Nitrilotris(benzene-4,1-diyl))tris(ethyne-2,1-diyl))-tris(quinoline-8,2-diyl))tris-(methylene) triacetate (19). To a solution of 8,8′,8″-((nitrilotris(benzene-4,1-diyl))tris(ethyne-2,1-diyl))tris(quinoline-2-carbaldehyde) **18** (53 mg, 67 μmol), in dry THF (2 mL), $NaBH_4$ was added (8.3 mg, 221.1 μmol). The reaction mixture was stirred overnight at room temperature. Then, DMAP (0.9 mg, 6.7 μmol) was added followed by the addition of a Ac_2O–Et_3N mixture (1 : 1, 0.6 mL). The reaction was stirred overnight at room temperature, quenched with an aqueous saturated $NaHCO_3$ solution and then extracted several times with CH_2Cl_2. The combined organic layer was dried (Na_2SO_4) and then concentrated under reduced pressure. The crude product was purified on silica gel (40% EtOAc in Petroleum Ether) to give (8,8′,8″-((nitrilotris(benzene-4,1-diyl))-tris(ethyne-2,1-diyl))tris(quinoline-8,2-diyl))tris(methylene) triacetate **19** (50 mg, 90%) as a yellow powder. ^{1}H NMR ($CDCl_3$, 400 MHz) δ (ppm): 8.18 (d, J = 8.5 Hz, 3H), 7.97 (dd, J = 7.2 Hz, J = 1.3 Hz, 3H), 7.79 (dd, J = 8.1 Hz, J = 1.3 Hz, 3H), 7.61 (d, J = 8.6 Hz, 6H), 7.49–7.54 (m, 6H), 7.16 (d, J = 8.6 Hz, 6H), 5.51 (s, 6H), 2.22 (s, 9H). ^{13}C NMR ($CDCl_3$, 100 MHz) δ (ppm): 21.2, 67.6, 87.2, 95.7, 118.4, 119.8, 123.6, 124.2, 126.3, 127.7, 128.0, 133.3, 134.1, 137.3, 147.0, 147.6, 157.0, 170.9. ESIHRMS: $C_{60}H_{42}N_4O_6$ calculated for $[M + H]^+$: 915.3177, found 915.3173.

(6,6′-((9,9-Bis(2-(2-(2-methoxyethoxy)ethoxy)ethyl)-9*H*-fluorene-2,7-diyl)bis(ethyne-2,1-diyl))bis(quinoline-6,2-diyl))-bis(methylene) diacetate (21). To a solution of 2,7-diiodo-9,9-bis[2-[2-(2-methoxyethoxy)ethoxy]ethyl]-9*H*-fluorene[17] **20** (142.1 mg, 200 μmol), (6-ethynylquinolin-2-yl)-methanol **3** (88 mg, 480 μmol), $PdCl_2(Ph_3P)_2$ (5.6 mg, 8 μmol), and CuI (3.1 mg, 16 μmol) in dry THF (2 mL) Et_3N (0.1 mL) was added. The reaction mixture was stirred overnight at room temperature, and then DMAP (2.5 mg, 20 μmol), and Ac_2O (57 μL, 600 μmol) were added. The reaction was stirred overnight at room temperature, quenched with an aqueous saturated $NaHCO_3$, and then extracted several times with EtOAc. The combined organic layer was dried and concentrated under reduced pressure. The crude product was purified on silica gel (eluent, EtOAc), to give 20 (172 mg, 95%) as a yellow powder. Mp: 85 °C. ^{1}H NMR ($CDCl_3$, 200 MHz) δ (ppm): 8.18 (d, J = 8.5 Hz, 2H), 8.03–8.12 (m, 4H), 7.86 (dd, J = 8.8 Hz, J = 1.6 Hz, 2H), 7.64–7.73 (m, 4H), 7.59 (dd, J = 7.8 Hz, J = 1.2 Hz, 2H), 7.51 (d, J = 8.4 Hz, 2H), 5.41 (s, 4H), 3.36–3.55 (m, 12H), 3.31 (s, 6H), 3.20–3.26 (m, 4H), 2.83 (t, J = 7.0 Hz, 4H), 2.45 (t, J = 7.0 Hz, 4H), 2.21 (s, 6H). ^{13}C NMR ($CDCl_3$, 100 MHz) δ (ppm): 21.1, 39.8, 51.6, 59.1, 67.0, 67.5, 70.2, 70.6, 72.0, 90.0, 91.6, 120.4, 121.8, 122.2, 126.7, 127.5, 129.6, 131.0, 131.4, 132.7, 136.8, 140.3, 147.2, 149.7, 157.0, 170.8. ESIHRMS: $C_{55}H_{56}N_2O_{10}$ calculated for $[M + Na]^+$: 927.3827, found 927.3795.

7-Hydroxycoumarin-4-ylmethyl acetate (CouOAc). 7-Hydroxycoumarin-4-ylmethyl acetate was synthesised by using the protocol reported by Furuta *et al.*[32a] To a stirred mixture of 4-chloromethyl-7-hydroxycoumarin[34] (1.0 g, 4.75 mmol) in toluene (48 mL) under an Argon atmosphere were added successively AcOH (0.8 mL, 14.3 mmol) and DBU (2.8 mL, 19 mmol). The reaction mixture was refluxed for 17 h. After being cooled down to room temperature, the mixture was concentrated under reduced pressure. The residue was diluted in CH_2Cl_2 then washed with a HCl solution (1N). The combined organic layers were dried (Na_2SO_4) and concentrated under reduced pressure. The resulting crude solid was washed with ether (10 mL) to give 0.84 g of 7-hydroxycoumarin-4-ylmethyl acetate (76%) as a yellow powder. Mp 148 °C. IR (KBr) ν (cm^{-1}): 3292.9, 3084.1, 2926.2, 1748.1, 1690.6, 1621.3, 1243.6. ^{1}H NMR (acetone-d_6, 200 MHz) δ (ppm): 7.59 (d, J = 8.8 Hz, 1H), 6.88 (dd, J = 8.8 Hz, J = 2.4 Hz, 1H), 6.78 (d, J = 2.4 Hz, 1H), 6.20 (t, J = 1.4 Hz, 1H), 5.33 (d, J = 1.4 Hz, 2H), 2.18 (s, 3H). ^{13}C NMR ($CDCl_3$, 50 MHz) δ (ppm): 21.6, 62.9, 104.7, 110.6, 111.7, 114.9, 127.5, 152.0, 157.6, 161.8, 163.3, 171.5. ESIHRMS: $C_{12}H_{10}O_5$ calculated for $[M + Na]^+$: 257.0420, found 257.0411. Anal. calcd for $C_{12}H_{10}O_5$: C, 61.54; H, 4.30; found: C, 61.18; H, 4.87.

Photophysical methods

All photophysical studies have been performed with freshly-prepared air-equilibrated solutions at room temperature (298 K). UV/Vis absorption spectra of 10^{-5} M solutions were recorded on a Jasco V-670 spectrophotometer. The reported molar extinction coefficients are within ±5%. Steady-state and time-resolved fluorescence measurements were performed on dilute solutions

(*ca.* 10^{-6} M, optical density < 0.1) contained in standard 1 cm quartz cuvettes using a Fluorolog spectrofluorometer. Emission spectra were obtained, for each compound, under excitation at the wavelength of the absorption maximum. Fluorescence quantum yields were measured according to literature procedures.[35] The reported fluorescence quantum yields are within ±5%. Fluorescence lifetimes were measured by time-correlated single photon counting (TCSPC). The reported lifetimes are within ±0.1 ns.

Two-photon absorption

2PA cross sections (σ_2) were determined from the two-photon excited fluorescence (TPEF) cross sections ($\sigma_2\Phi$) and the fluorescence emission quantum yield (Φ). TPEF cross sections of 10^{-4} M solutions were measured relative to fluorescein in 0.01M aqueous NaOH for 715–980 nm,[28] using the well-established method described by Xu and Webb[28a] and the appropriate solvent-related refractive index corrections.[36] Reference values between 700 and 715 nm for fluorescein were taken from literature.[23] The quadratic dependence of the fluorescence intensity on the excitation power was checked for each sample and all wavelengths. Measurements were conducted using an excitation source delivering fs pulses. This allows avoiding excited-state absorption during the pulse duration, a phenomenon which has been shown to lead to overestimated 2PA cross-section values.[7] To span the 700–980 nm range, a Nd:YLF-pumped Ti:sapphire oscillator was used generating 150 fs pulses at a 76 MHz rate. The excitation was focused into the cuvette through a microscope objective (10×, NA 0.25). The fluorescence was detected in epifluorescence mode *via* a dichroic mirror (Chroma 675dcxru) and a barrier filter (Chroma e650sp-2p) by a compact CCD spectrometer module BWTek BTC112E. Total fluorescence intensities were obtained by integrating the corrected emission. The experimental uncertainty on the absolute action cross-sections determined by this method has been estimated to be ±10%.

Photolysis measurements

A solution of compound **6** (1.65 mg, 3.52 μmol, 1.1×10^{-4} M), in a mixture 21 mL–10 mL THF–buffer solution (pH 7.00), was irradiated using two lamps of 365 nm (2×6 W). Between each duration, a small aliquot (0.5 mL) of the solution was removed and diluted with a solution of ammonium formate (5% in MeOH w/w). The photolysis was followed by reversed-phase HPLC-MS analysis eluted with a gradient mixture of methanol and water using absorbance detection at 254 nm or 365 nm. The ratio was estimated by analysis of the HPLC chromatogram, the mass completed the analysis to confirm the authenticity of the products. The reported uncaging quantum yields are within ±3%.

We also noticed that the photosensitive dipolar molecules and the remnant alcohols display similar ε values at 365 nm. In fact, only the conjugated triphenylamine–quinoline chromophore is responsible for the absorption ability of the compounds at this wavelength as carbonyl groups do not absorb light at 365 nm. Thus, no correction is necessary for HPLC analysis with detection at 365 nm. Integration ratios of the peaks related to the photosensitive molecule and the remnant alcohol correspond exactly to concentration ratios. This observation proved to be crucial for our investigations when THF was used.

Acknowledgements

This work was supported by a grant from Agence Nationale pour la Recherche (Grant 2010 ANR-10-BLAN-1436). MBD gratefully thanks the Conseil Régional d'Aquitaine for generous funding (Chaire d'Accueil grant). We thank M. Klausen (ISM, Université Bordeaux 1) for his contribution to CouOAc synthesis.

Notes and references

1 P. Klán, T. Šolomek, C. G. Bochet, A. Blanc, R. Givens, M. Rubina, V. Popik, A. Kostikov and J. Wirz, *Chem. Rev.*, 2013, **113**, 119–191 and references cited therein.

2 (*a*) C. G. Bochet, *J. Chem. Soc., Perkin Trans. 1*, 2002, 125–142; (*b*) R. S. Givens, P. G. I. Conrad, A. L. Yousef and J.-I. Lee, in *CRC Handbook of Organic Photochemistry and Photobiology*, ed. W. M. Horspool, 2nd edn, 2003, pp. 69.1–69.46.

3 C. G. Bochet, *Synlett*, 2004, 2268–2274.

4 (*a*) A. P. Pelliccioli and J. Wirz, *Photochem. Photobiol. Sci.*, 2002, **1**, 441–458; (*b*) G. Mayer and A. Heckel, *Angew. Chem., Int. Ed.*, 2006, **45**, 4900–4921; (*c*) H. Yu, J. Li, D. Wu, Z. Qiu and Y. Zhang, *Chem. Soc. Rev.*, 2010, **39**, 464–473; (*d*) C. Brieke, F. Rohrbach, A. Gottschalk, G. Mayer and A. Heckel, *Angew. Chem., Int. Ed.*, 2012, **51**, 8446–8476; (*e*) T. M. Dore and H. C. Wilson, *Neuromethods*, 2011, **55**, 57–92; (*f*) G. Bort, T. Gallavardin, D. Ogden and P. I. Dalko, *Angew. Chem., Int. Ed.*, 2013, **52**, 4526–4537.

5 N. Kiskin, R. Chillingworth, J. McCray, D. Piston and D. Ogden, *Eur. Biophys. J.*, 2002, **30**, 588–604.

6 (*a*) I. Aujard, C. Benbrahim, M. Gouget, O. Ruel, J.-B. Baudin, P. Neveu and L. Jullien, *Chem.–Eur. J.*, 2006, **12**, 6865–6879; (*b*) L. Donato, A. Mourot, C. M. Davenport, C. Herbivo, D. Warther, J. Léonard, F. Bolze, J.-F. Nicoud, R. H. Kramer, M. Goeldner and A. Specht, *Angew. Chem., Int. Ed.*, 2012, **51**, 1840–1843; (*c*) A. Specht, F. Bolze, L. Donato, C. Herbivo, S. Charon, D. Warther, S. Gug, J.-F. Nicoud and M. Goeldner, *Photochem. Photobiol. Sci.*, 2012, **11**, 578–586.

7 (*a*) G. S. He, L.-S. Tan, Q. Zheng and P. N. Prasad, *Chem. Rev.*, 2008, **108**, 1245–1330; (*b*) F. Terenziani, C. Katan, E. Badaeva, S. Tretiak and M. Blanchard-Desce, *Adv. Mater.*, 2008, **20**, 4641–4678; (*c*) H. M. Kim and B. R. Cho, *Chem. Commun.*, 2009, 153–164; (*d*) M. Pawlicki, H. A. Collins, R. G. Denning and H. L. Anderson, *Angew. Chem., Int. Ed.*, 2009, **48**, 3244–3266.

8 S. Gug, F. Bolze, A. Specht, C. Bourgogne, M. Goeldner and J.-F. Nicoud, *Angew. Chem., Int. Ed.*, 2008, **47**, 9525–9529.

9 (*a*) S.-J. Chung, K.-S. Kim, T.-C. Lin, G. S. He, J. Swiatkiewicz and P. N. Prasad, *J. Phys. Chem. B*, 1999, **103**, 10741–10745; (*b*) L. Porr''s, O. Mongin, C. Katan, M. Charlot, T. Pons,

J. Mertz and M. Blanchard-Desce, *Org. Lett.*, 2004, **6**, 47–50; (*c*) C. Le Droumaguet, O. Mongin, M. H. V. Werts and M. Blanchard-Desce, *Chem. Commun.*, 2005, 2802–2804; (*d*) J. C. Collings, S.-Y. Poon, C. Le Droumaguet, M. Charlot, C. Katan, L.-O. Pålsson, A. Beeby, J. A. Mosely, H. M. Kaiser, W.-Y. Wong, M. Blanchard-Desce and T. B. Marder, *Chem.–Eur. J.*, 2009, **15**, 198–208; (*e*) P. Hrobárik, V. Hrobáriková, I. Sigmundová, P. Zahradník, M. Fakis, I. Polyzos and P. Persephonis, *J. Org. Chem.*, 2011, **76**, 8726–8736; (*f*) C. Rouxel, C. Le Droumaguet, Y. Macé, S. Clift, O. Mongin, E. Magnier and M. Blanchard-Desce, *Chem.–Eur. J.*, 2012, **18**, 12487–12497.

10 (*a*) D. Beljonne, W. Wenseleers, E. Zojer, Z. Shuai, H. Vogel, S. J. K. Pond, J. W. Perry, S. R. Marder and J. L. Brédas, *Adv. Funct. Mater.*, 2002, **12**, 631–641; (*b*) C. Katan, F. Terenziani, O. Mongin, M. H. V. Werts, L. Porr''s, T. Pons, J. Mertz, S. Tretiak and M. Blanchard-Desce, *J. Phys. Chem. A*, 2005, **109**, 3024–3037.

11 (*a*) O. D. Fedoryak and T. M. Dore, *Org. Lett.*, 2002, **4**, 3419–3422; (*b*) Y. Zhu, C. M. Pavlos, J. P. Toscano and T. M. Dore, *J. Am. Chem. Soc.*, 2006, **128**, 4267–4276; (*c*) M. J. Davis, C. H. Kragor, K. G. Reddie, H. C. Wilson, Y. Zhu and T. M. Dore, *J. Org. Chem.*, 2009, **74**, 1721–1729; (*d*) H.-Y. An, C. Ma, J. L. Nganga, Y. Zhu, T. M. Dore and D. L. Phillips, *J. Phys. Chem. A*, 2009, **113**, 2831–2837; (*e*) H.-Y. An, C. Ma, W. Li, K. T. Harris, T. M. Dore and D. L. Phillips, *J. Phys. Chem. A*, 2010, **114**, 2498–2505; (*f*) J. Ma, S. C. Cheng, H. An, M.-D. Li, C. Ma, A. C. Rea, Y. Zhu, J. L. Nganga, T. M. Dore and D. L. Phillips, *J. Phys. Chem. A*, 2011, **115**, 11632–11640; (*g*) J. Ma, A. C. Rea, H. An, C. Ma, X. Guan, M.-D. Li, T. Su, C. S. Yeung, K. T. Harris, Y. Zhu, J. L. Nganga, O. D. Fedoryak, T. M. Dore and D. L. Phillips, *Chem.–Eur. J.*, 2012, **18**, 6854–6865; (*h*) M. Petit, C. Tran, T. Roger, T. Gallavardin, H. Dhimane, F. Palma-Cerda, M. Blanchard-Desce, F. C. Acher, D. Ogden and P. I. Dalko, *Org. Lett.*, 2012, **14**, 6366–6369.

12 P. Dalko, M. Petit, D. Ogden and F. Acher, *WO Pat.*, WO2011086469A1, 2011.

13 C. Wang, L.-O. Pålsson, A. S. Batsanov and M. R. Bryce, *J. Am. Chem. Soc.*, 2006, **128**, 3789–3799.

14 Y. Shirota, T. Kobata and N. Noma, *Chem. Lett.*, 1989, 1145–1148.

15 F. Xu, L. Peng, A. Orita and J. Otera, *Org. Lett.*, 2012, **14**, 3970–3973.

16 (*a*) O. Mongin, L. Porr''s, L. Moreaux, J. Mertz and M. Blanchard-Desce, *Org. Lett.*, 2002, **4**, 719–722; (*b*) O. Mongin, L. Porr''s, M. Charlot, C. Katan and M. Blanchard-Desce, *Chem.–Eur. J.*, 2007, **13**, 1481–1498.

17 D. Brevet, L. Raehm, M. Blanchard-Desce, O. Mongin, M. Gary-bobo-sable-Teychene, M. Garcia, A. Morere and J.-O. Durand, *WO Pat.*, WO2011073054A1, 2011.

18 These values are related to σ_R values, see: C. Hansch, A. Leo and R. W. Taft, *Chem. Rev.*, 1991, **91**, 165–195.

19 Using a simple excitonic coupling picture, we can derive a coupling value of about 0.15 eV and 0.13 eV for octupolar derivatives having 6-quinoline and 8-quinoline moieties respectively.

20 S. J. Strickler and R. A. Berg, *J. Chem. Phys.*, 1962, **37**, 814–822.

21 The smaller blue shift observed for 8-quinoline derivatives is consistent with smaller $\Delta\mu$ values.

22 F. Terenziani, A. Painelli, C. Katan, M. Charlot and M. Blanchard-Desce, *J. Am. Chem. Soc.*, 2006, **128**, 15742–15755.

23 C. Katan, S. Tretiak, M. H. V. Werts, A. J. Bain, R. J. Marsh, N. Leonczek, N. Nicolaou, E. Badaeva, O. Mongin and M. Blanchard-Desce, *J. Phys. Chem. B*, 2007, **111**, 9468–9483.

24 C. Katan, M. Charlot, O. Mongin, C. l. Le Droumaguet, V. Jouikov, F. Terenziani, E. Badaeva, S. Tretiak and M. Blanchard-Desce, *J. Phys. Chem. B*, 2010, **114**, 3152–3169.

25 (*a*) E. Lippert, *Z. Naturforsch., A: Phys. Sci.*, 1955, **10**, 541–545; (*b*) N. Mataga, Y. Kaifu and M. Koizumi, *Bull. Chem. Soc. Jpn.*, 1955, **28**, 690–691.

26 For three-branch derivatives, excitation hopping between branches prevents the use of anisotropy data for the estimation of cavity radius values.

27 J. R. Lakowicz, *Principles of Fluorescence Spectroscopy*, Kluwer Academic/Plenum Publishers, New York, 1999.

28 (*a*) C. Xu and W. W. Webb, *J. Opt. Soc. Am. B*, 1996, **13**, 481–491; (*b*) M. A. Albota, C. Xu and W. W. Webb, *Appl. Opt.*, 1998, **37**, 7352–7356.

29 Y. Laras, V. Hugues, Y. Chandrasekaran, M. Blanchard-Desce, F. C. Acher and N. Pietrancosta, *J. Org. Chem.*, 2012, **77**, 8294–8302.

30 (*a*) M. Barzoukas and M. Blanchard-Desce, *J. Chem. Phys.*, 2000, **113**, 3951–3959; (*b*) M. Rumi, J. E. Ehrlich, A. A. Heikal, J. W. Perry, S. Barlow, Z.-Y. Hu, D. McCord-Maughon, T. C. Parker, H. Röckel, S. Thayumanavan, S. R. Marder, D. Beljonne and J.-L. Brédas, *J. Am. Chem. Soc.*, 2000, **122**, 9500–9510.

31 C. Rouxel, M. Charlot, O. Mongin, T. R. Krishna, A.-M. Caminade, J.-P. Majoral and M. Blanchard-Desce, *Chem.–Eur. J.*, 2012, **18**, 16450–16462.

32 (*a*) T. Furuta, S. S. H. Wang, J. L. Dantzker, T. M. Dore, W. J. Bybee, E. M. Callaway, W. Denk and R. Y. Tsien, *Proc. Natl. Acad. Sci. U. S. A.*, 1999, **96**, 1193–1200; (*b*) M. Lu, O. D. Fedoryak, B. R. Moister and T. M. Dore, *Org. Lett.*, 2003, **5**, 2119–2122.

33 S. Gug, S. Charon, A. Specht, K. Alarcon, D. Ogden, B. Zietz, J. Léonard, S. Haacke, F. Bolze, J.-F. Nicoud and M. Goeldner, *ChemBioChem*, 2008, **9**, 1303–1307.

34 W. Garner, M. Garner and R. D. Blum, *WO Pat.*, WO2009111633A2, 2009.

35 (*a*) J. N. Demas and G. A. Crosby, *J. Phys. Chem.*, 1971, **75**, 991–1024; (*b*) D. F. Eaton, *Pure Appl. Chem.*, 1988, **60**, 1107–1114.

36 M. H. V. Werts, N. Nerambourg, D. Pélégry, Y. Le Grand and M. Blanchard-Desce, *Photochem. Photobiol. Sci.*, 2005, **4**, 531–538.